

CTR (Misc)

Reese
#72

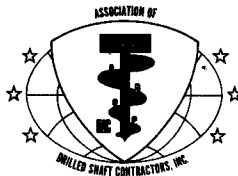
Keith Le Ger

LOAD TESTS OF INSTRUMENTED DRILLED SHAFTS CONSTRUCTED BY THE SLURRY DISPLACEMENT METHOD

By

Lymon C. Reese and Fadlo T. Touma

Furnished by:



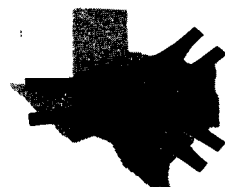
**Association of
Drilled Shaft Contractors, Inc.**

P. O. BOX 47482, DALLAS, TEXAS 75247

RESEARCH REPORT
INTERAGENCY CONTRACT 108
with the
TEXAS HIGHWAY DEPARTMENT

CENTER FOR HIGHWAY RESEARCH
THE UNIVERSITY OF TEXAS AT AUSTIN

JANUARY 1972



**For Loan Only:
CTR Library**

LOAD TESTS OF INSTRUMENTED DRILLED SHAFTS
CONSTRUCTED BY THE SLURRY
DISPLACEMENT METHOD

By

Lymon C. Reese and Fadlo T. Touma

RESEARCH REPORT
INTERAGENCY CONTRACT 108
with the
TEXAS HIGHWAY DEPARTMENT

JANUARY 1972

LOAD TESTS OF INSTRUMENTED DRILLED SHAFTS
CONSTRUCTED BY THE SLURRY DISPLACEMENT METHOD

by

Lymon C. Reese

Fadlo T. Touma

Research Report

Interagency Contract 108

Research Project

conducted for

The Texas Highway Department

by the

CENTER FOR HIGHWAY RESEARCH
THE UNIVERSITY OF TEXAS AT AUSTIN

January 1972

PREFACE

This report is concerned with research performed by the Center for Highway Research under the terms of Interagency Contract 108 between the Center for Highway Research and the Texas Highway Department. The report describes the construction, instrumentation, and testing of three drilled shafts which had been constructed by the "slurry displacement method." The observed test data were analyzed and the load transfer evaluated for the different soil layers.

The cooperation and the combined efforts of many persons made this work possible. The technical assistance of Dr. Michael W. O'Neill, Messrs. Harold H. Dalrymple, Frederick E. Koch, and James N. Anagnos is appreciated. The patience of Mrs. Mary E. Sargeant who typed the manuscript is greatly appreciated.

The Texas Highway Department contract representatives Mr. H. D. Butler and Mr. Horace Hoy have been helpful and cooperative in the development of the work. Special acknowledgement is given to officials of the Houston Urban Office whose progressive approach to engineering problems made this work possible. Mr. Gaston P. Berthelot and his office personnel are due special thanks for their valuable contributions and efforts.

Lymon C. Reese
Fadlo T. Touma

January 1972

ABSTRACT

The use of drilled shafts in stiff clays where the drilled holes can stand open without any lateral support has met with great success in the last several years. This success has motivated drilling contractors to attempt to extend the use of drilled shafts to other types of soils, such as water-bearing sand and gravel, and to devise new construction procedures to meet the difficulties encountered when drilling in such soils. The "slurry displacement method" is one recent procedure that has been used successfully in constructing drilled shafts in several places around the world.

The Center for Highway Research has previously conducted an intensive research on drilled shafts in stiff clays and undertook recently to cooperate with the Texas Highway Department in instrumenting, constructing, and testing three drilled shafts constructed by the "slurry displacement method."

This report is concerned with the description of the work done by the Center for Highway Research. Included are a description of the instrumentation, the construction, and the testing of three shafts. The data obtained from the measuring instruments are analyzed, and values of load transfer in different soil layers are obtained. These values are compared with values of load transfer obtained from previous tests in similar soils on shafts constructed in the dry.

SUMMARY

Three drilled shafts have been constructed using the slurry displacement method where the mud slurry used to stabilize the hole is directly displaced by tremie concrete.

This report is concerned with the instrumentation, construction, and testing of these shafts. The shafts varied between 30 and 36 inches in diameter and the penetration was from 45 to 76 feet. The soil profiles include stiff clays and water-bearing sands. The shafts were equipped with Mustran load cells. Several quick-load tests were conducted on the shafts, and the data from the load tests and the instrumentation was analyzed.

From the study it was found that:

1. the values of load transfer developed in clayey soils on the sides of the shaft constructed by the slurry displacement method are comparable to those developed in shafts constructed in the dry;
2. the condition of the shaft is influenced considerably by the construction technique.

TABLE OF CONTENTS

	Page No.
PREFACE.	ii
ABSTRACT	iii
SUMMARY.	iv
INTRODUCTION	1
CHAPTER I - DESCRIPTION OF WORK	
Soil Exploration	2
Instrumentation.	2
Installation of Shafts	6
Loading of Shafts.	8
Extraction of Shafts	9
CHAPTER II - RESULTS AND OBSERVATIONS	
Results of Tests	11
Discussion of Results.	33
General Field Observations	42
REFERENCES	46
APPENDICES	
Appendix I - Boring Logs	47
Appendix II - Test Shafts Design Sheets.	55

LIST OF FIGURES

	Page No.
Fig. 1 - Generalized Elevation for Test Shafts	3
Fig. 2 - Soil Profile and Sketches of Location of Shaft Instrumentation	4
Fig. 3 - Shear Strength from Transmatic Triaxial Test.	12
Fig. 4 - United States Bureau of Reclamation Charts (Gibbs and Holtz)	14
Fig. 5 - Shear Strength Profile, G1.	17
Fig. 6a - Load-Settlement Curves, G1 - Test 1.	18
Fig. 6b - Load-Settlement Curves, G1 - Test 2.	19
Fig. 6c - Load-Settlement Curves, G1 - Test 3.	20
Fig. 7 - Load-Distribution Curves, G1 - Test 1	21
Fig. 8 - Load Transfer Curves, G1 - Test 1	22
Fig. 9 - Shear Strength Profile, G2.	23
Fig. 10a - Load-Settlement Curves, G2 - Test 1	24
Fig. 10b - Load-Settlement Curve, G2 - Test 2.	25
Fig. 11 - Load-Distribution Curve, G2 - Test 1	26
Fig. 12 - Load Transfer Curves, G2 - Test 1.	27
Fig. 13 - Shear Strength Profile, BB	28
Fig. 14a - Load-Settlement Curves, BB - Test 1	29
Fig. 14b - Load-Settlement Curves, BB - Test 2	30
Fig. 14c - Load-Settlement Curves, GG - Test 3	30
Fig. 15 - Load-Distribution Curves, BB - Test 1.	31
Fig. 16 - Load Transfer Curves, BB - Test 1.	32

LIST OF TABLES

	Page No.
Table 1 - Location and Geometric Descriptions of Test Shafts . .	3
Table 2 - Depths and Diameters of Shafts at Gages Locations. . .	5
Table 3 - Dates and General Information on Load Tests.	10
Table 4 - Correlations Between Load Transfer and Shear Strength.	34
Table 5 - Correlations Between Load Transfer and Shear Strength.	35
Table 6 - Correlations Between Load Transfer and Shear Strength.	36
Table 7 - Summary of Results on Correlation Factors.	37
Table 8 - Measured Tip Resistance.	37
Table 9 - Correlations Between Load Transfer and Shear Strength From Previous Research	41

INTRODUCTION

The construction of drilled shafts presents several technical problems and becomes very expensive when penetration of caving soils is required. A common procedure followed in such soils is to install a temporary casing to seal the caving layers. This casing could be installed in a hole already stabilized by mud (procedure followed by some contractors in Texas) or it may be driven by an impact or vibratory hammer and then cleaned out. A procedure that has been used extensively around the world in the last two decades consists of stabilizing the hole with a mud slurry during drilling and then placing tremie concrete under the mud.

Engineers of the Houston Urban Office, thinking of implementing this latter method, designed load tests on three drilled shafts constructed by this method, which shall be referred to as the "slurry displacement method."

The Center for Highway Research, under the terms of the Interagency Contract 108, cooperated with the Texas Highway Department in instrumenting and testing these shafts.

This report describes briefly the work done by the CFHR, discusses the main findings of the research, and gives correlations between load transfer and the shear strength as measured by the transmatic triaxial test, the THD cone penetrometer test, and the standard penetration test (SPT).

CHAPTER 1

DESCRIPTION OF WORK

The test shafts were located within the city limits of Houston. The specific location and geometrical description of the test shafts are given in Table 1 and Fig. 1. Figure 2 shows soil profiles and sketches of the location of the instrumentation at each of the three sites. Table 2 gives the depths at various gages levels as well as the diameter of the shaft at those levels as measured after extraction. In the following sections a general description of the work is given.

Soil Exploration

In addition to the preliminary borings made at the test sites, three borings were made close to each shaft location. Undisturbed samples for the transmatic triaxial test were taken from one boring, and standard penetration tests and THD cone penetrometer tests were run in the other two. Pocket penetrometer tests were made on relatively intact samples from all three holes. The boring logs are shown in the Appendix.

Instrumentation

The instrumentation of the shafts consisted mainly of Mustran load cells developed by the Center for Highway Research (Barker and Reese, 1969). Two perpendicular planes through the shaft axis were selected for cell installation, with the Mustran cells being used in pairs in a given plane. The cells were placed inside the cage formed by the reinforcing steel. At most levels only two cells were installed, both in the same plane. Four cells were used at the top and bottom levels. (See Fig. 2.)

TABLE 1 - LOCATION AND GEOMETRIC DESCRIPTIONS OF TEST SHAFTS

Shaft	Location	d_n , in.	d_a , in.	D_b , ft.	D_e , ft.	D_t , ft.
G1	South middle bay of bent 12 of I 610-145 Interchange East-bound structure	36	37.7	54.8	7.0	61.8
G2	North bay of bent 27 of I 610-145 Interchange East-bound structure*	30	31.4	73.5	5.5	79.0
BB	West bay of bent 5 of left frontage street SH 288 and Brays Bayou structure.	30	31.4	45.0	3.0	48.0

*Originally planned in the south bay but a first attempt to install it in that bay failed.

D_e = exposed height of shaft

D_b = buried height of shaft

D_t = $D_e + D_b$ (Total height of shaft)

d_n = nominal diameter (or sonotube diameter)

d_a = average measured diameter

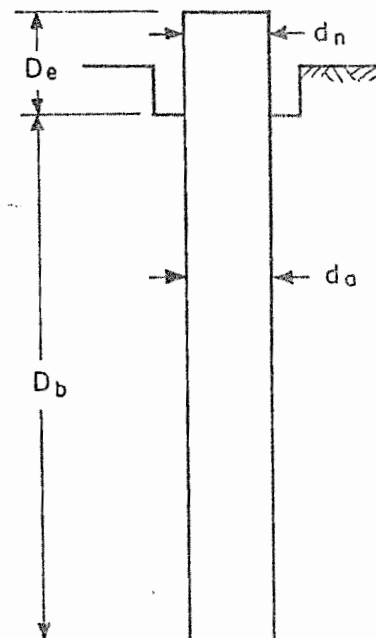
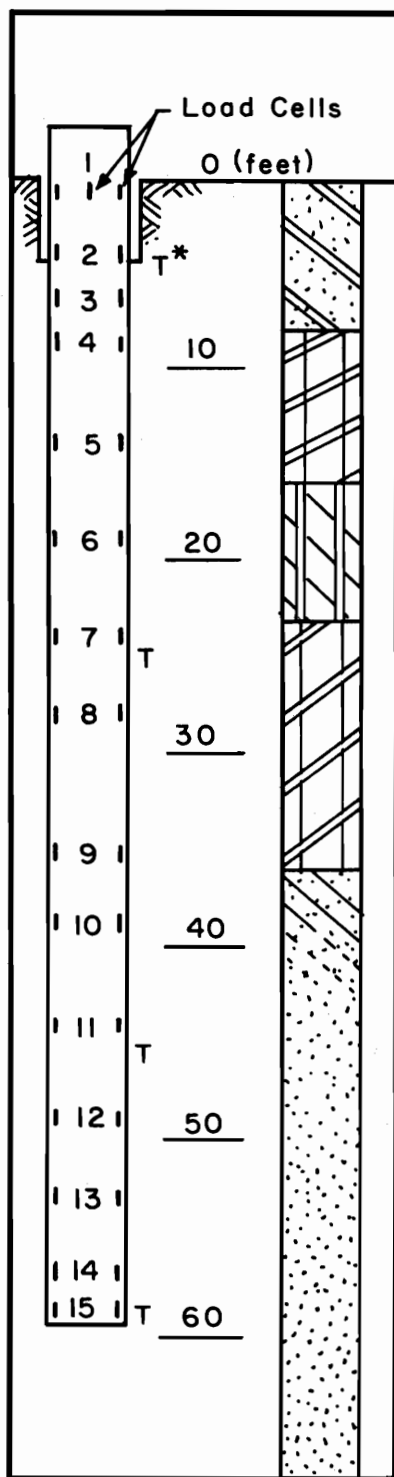
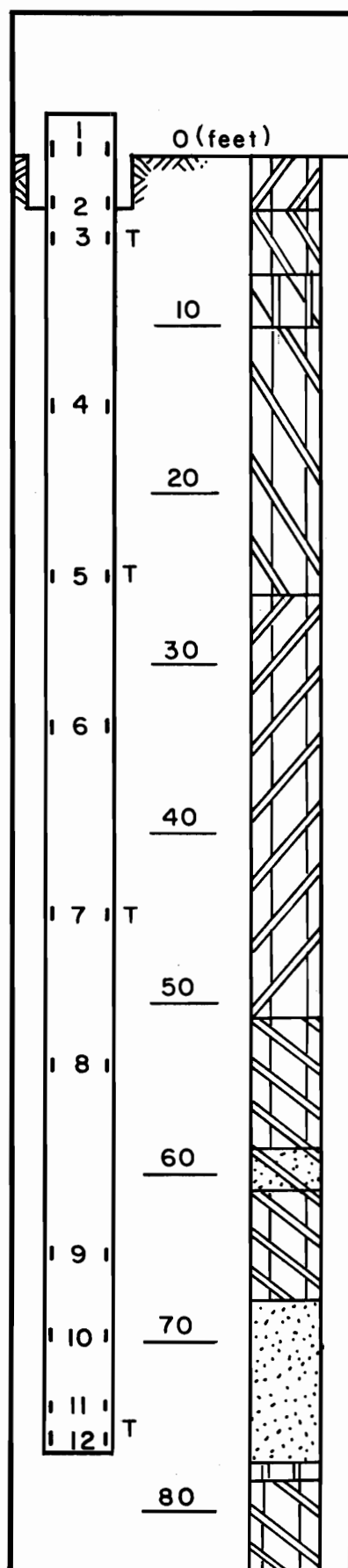


Fig. 1 Generalized Elevation
for Test Shafts

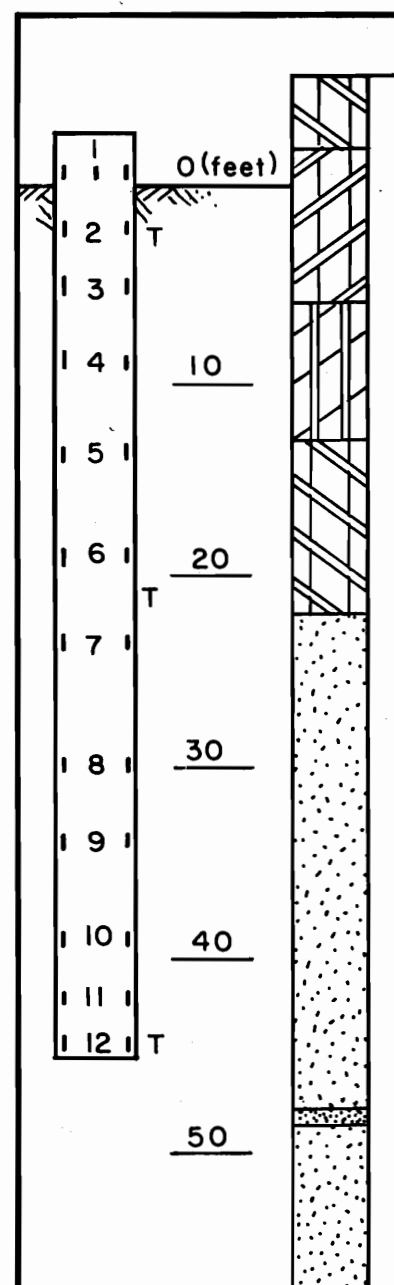


(a) G1 Site

* T = Thermocouple



(b) G2 Site



(c) BB Site

Fig. 2 Soil Profiles and Sketches of Location of Shaft Instrumentation

TABLE 2. DEPTHS AND DIAMETERS OF SHAFTS AT GAGE LOCATIONS

Shaft G1			Shaft G2			Shaft BB		
level	depth* (ft)	diameter (in)	level	depth* (ft)	diameter (in)	level	depth* (ft)	diameter (in)
1	3.7	36.0	1	2.5	30.0	1	2.7	30.0
2	6.7	38.0	2	5.5	32.0	2	5.2	31.2
3	9.2	37.6	3	7.5	31.7	3	8.6	31.1
4	11.7	37.6	4	17.5	31.4	4	12.0	31.3
5	16.7	37.6	5	27.5	31.3	5	17.0	--
6	21.7	37.7	6	36.3	31.6	6	22.2	31.5
7	26.8	37.4	7	47.4	31.3	7	27.0	32.0
8	30.7	37.4	8	56.4	31.6	8	33.2	31.6
9	37.9	37.5	9	67.5	31.4	9	37.1	--
10	41.6	37.4	10	72.4	31.6	10	42.2	31.3
11	46.7	38.0	11	76.5	31.3	11	45.0	31.0
12	51.7	38.6	12	78.8	31.1	12	47.4	25.2
13	55.9	38.6						
14	59.5	37.6						
15	61.5	36.8						

*Depths are measured from the butt of the shaft.

The spacing of the gages was based on the following considerations:

1. To get more information from sand layers because clay was the subject of previous intensive research,
2. To insure a good calibration level at the top of each shaft,
3. To obtain an accurate measurement of the tip resistance.

Thermocouples to measure temperature variations during curing were installed at three or four levels in each shaft.

Installation of Shafts

The procedure which was followed in the installation of the shafts, except for minor variations, was as follows:

1. Open a hole in the dry until a water-bearing, caving layer was encountered.
2. Immediately introduce the premixed mud slurry and keep it at a level within three to five feet of the ground surface.
3. Continue drilling to plan elevation under mud slurry.
4. Clean the bottom of the hole with a bucket or an auger immediately before the reinforcing steel cage is set in place.
5. Attach four concrete blocks at the cage bottom to avoid sinking of the cage in the sand, and then seat it in the hole.
6. Insert a temporarily sealed tremie ten inches in diameter through guides welded to the reinforcing steel cage and seat it in the hole.

7. Fill the tremie with concrete, and unplug it by lifting it up.
8. Place concrete while keeping the tremie tip well embedded in the concrete and helping the flow out by lifting the tremie as the concrete bucket is emptied.
9. Waste the first portion of the concrete flow, as this concrete is usually contaminated with mud, and then form the top three to five feet of the shaft with a sonotube.

The following are some particular observations at the installation of each shaft.

G1: Cleaning of the hole with an auger was unsuccessful. Cuttings and loose soil were believed to have fallen back to the bottom. As the site was muddy and the top of the hole was not protected, the workmen caused soft mud to fall into the hole while walking around the shaft. The belief that soft material was deposited at the hole bottom was later sustained by the fact that the tremie sunk about six inches when the first bucket of concrete was poured into the tremie.

G2: A first attempt to install the shaft in the south bay of the bent failed because the contractor did not keep the mud slurry at a high enough level in the hole. Keeping the mud slurry near the level of the caving soils accelerated the caving because of the scouring action caused by the fluctuation of the mud surface. The first hole was filled with concrete and abandoned.

The second attempt was successful because the mud slurry was kept near the ground surface. Also, premixed mud slurry was used, a procedure which was found advantageous. In-hole mixing as used during the first attempt could have aided the scour and the caving which was observed.

The bottom of the hole was cleaned with a bucket just before the steel cage was introduced. Unusually nonhomogeneous soil conditions existed at the site, and there was uncertainty about the character of the soil at the tip of the shaft.

BB: Two observations were made concerning the mud at this site:

- a. The mud slurry was too thick because some water drained out of the hole leaving a thick bentonite gel.
- b. Contaminated water from Brays Bayou was used in mixing the mud. This contaminated water caused flocculation of the bentonite and inhibited the formation of the mud cake.

Soil borings at the site indicated that the sand formation contained occasional sandstone lenses. At the shaft location these lenses were not encountered; however, a 10-inch auger advanced in the sand below plan tip elevation indicated hard layers interpreted as sandstone 2.5 feet below the tip. No particular effort was made to clean the hole, as it was intended to allow loose sediments to remain at the bottom.

Loading of Shafts

In all but one test, the quick-test procedure, prescribed by the Texas Highway Department, "Special Provisions to Specifications Item 405, 1965," was used. The third load test on the G1 test shaft was of the cyclic type,

as described in Barker and Reese, 1970. Table 3 shows the dates of the tests, the load increments used, and the ultimate loads applied. It should be noted that shaft BB was tested at an early age of 16 days to learn about the effect of age on the capacity of drilled shafts.

Extraction of Shafts

The three shafts were extracted after test-loading was finished. The extraction was accomplished by drilling an annular opening around the shaft to the depth of the test shaft. The shaft was loosened using a large block-and-tackle frame, and then extracted easily with the rig cable. The operation encountered difficulties at the G2 site where the annular opening kept sloughing and had to be protected by a large casing.

When a shaft was removed from the soil its length and diameter at each of the gages levels were measured. The soil-concrete interface was carefully examined by studying original soil still adhering to the shaft surface. Some Mustran cells were exposed by use of a jack hammer to observe their seating conditions in the concrete. In removing the cells, concrete was examined for possible mud slurry contamination.

TABLE 3. DATES AND GENERAL INFORMATION ON LOAD TESTS

Shaft	Test	Date of Test	Load Incr.	Unloading Incr.	Maximum Load Applied
BB	1	10- 7-71	25T	--*	750T
Cast 9-2-71	2	10- 8-71	50T	75T	750T
Extracted 10-13-71	3	10- 8-71	100T	300T	600T
G2	1	10-12-71	25T	50T	700T
Cast 8-14-71	2	10-12-71	50T	100T	680T
Extracted 10-26-71					
G1	1	10-19-71	25T	50T	480T
Cast 9-3-71	2	10-19-71	50T	100T	450T
Extracted 11-5-71	3(Cyclic)	10-19-71	75T	one incr.	450T

*Hydraulic system broke and an unloading curve could not be obtained.

CHAPTER II

RESULTS AND OBSERVATIONS

Results of Tests

The results of the tests on each shaft are presented as follows:

A. Shear Strength Profile

Shear strength profiles, as plotted in Figures 5, 9, and 13, were obtained using the following testing methods:

1. The transmatic triaxial test
2. The THD cone penetrometer
3. The standard penetration test (SPT)
4. The pocket penetrometer

The transmatic triaxial test yields for each tested soil specimen a Mohr envelope (Fig. 3) from which the shear strength is evaluated by the expression:

$$s = c + \bar{p} \tan \phi$$

where

s = shear strength (T/ft^2)

c = cohesion (T/ft^2) as given by the Mohr envelope

\bar{p} = effective overburden pressure (T/ft^2)

ϕ = friction angle as given by the Mohr envelope.

The THD cone penetrometer blow count is correlated with the shear strength of soils in charts shown in the Foundation Manual of the Texas Highway Department (1964). Values of shear strength from the triaxial transmatic test and the THD cone penetrometer test were obtained from the design sheets prepared by the Houston Urban Office (Appendix).

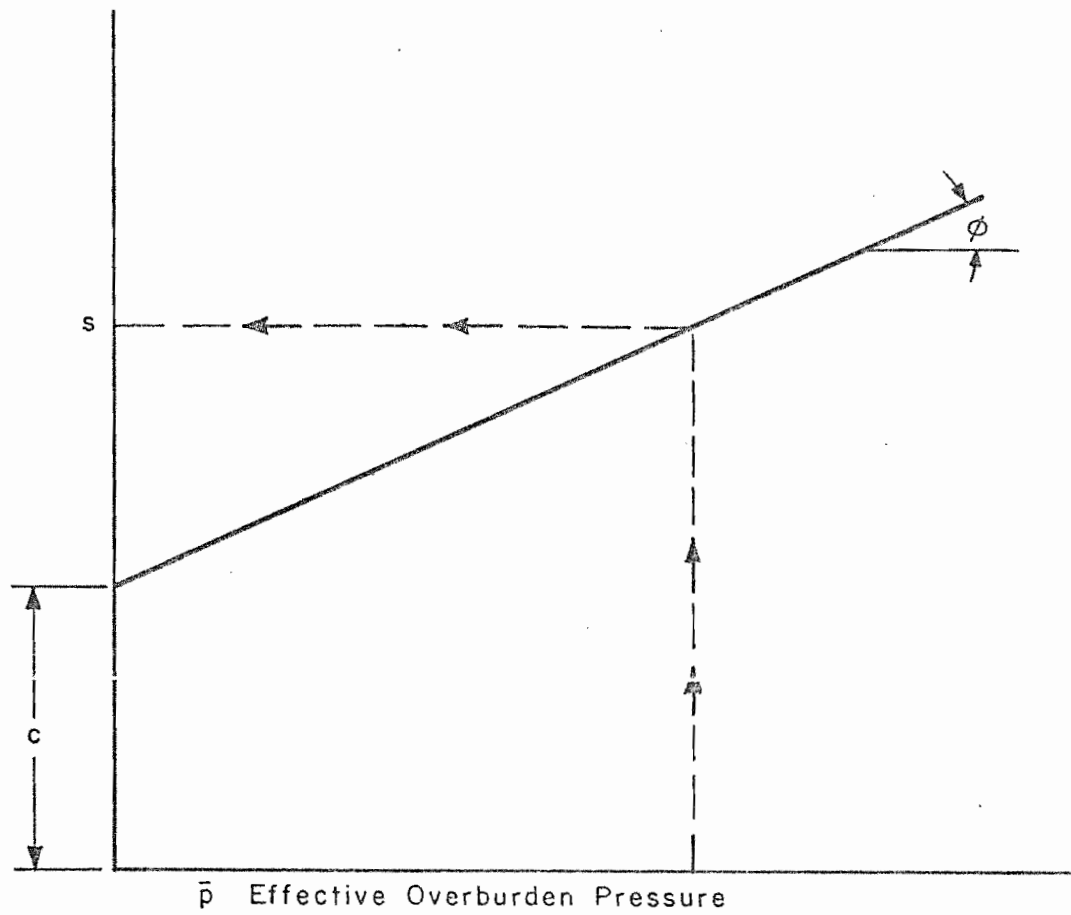


Fig. 3 Shear Strength from Transmatic Triaxial Test

The shear strength as obtained from the standard penetration test can be expressed for clays as:

$$s(T/ft^2) = \frac{N}{15} \quad (\text{Terzaghi and Peck})$$

where

N = Number of blows per foot of penetration.

The shear strength for sands is given by the following expression:

$$s = \bar{p} \cdot \tan \bar{\phi}$$

where

$\bar{\phi}$ = estimated for the relative density given by the U.S.B.R. charts (Gibbs and Holtz) and shown in Fig. 4.

The pocket penetrometer values of shear strength are obtained by a "Soil Test" Penetrometer from measurements taken on relatively intact samples in the field.

Also, some of the soil samples were tested by the UT triaxial procedure (O'Neill and Reese, 1970), and the results are plotted on the shear strength profile. These results are not conclusive because some of the samples failed on slickensides and fissures. It was established earlier that a large number of samples is needed for this test to allow a consideration of a statistical average of the shear strength (O'Neill and Reese, 1970).

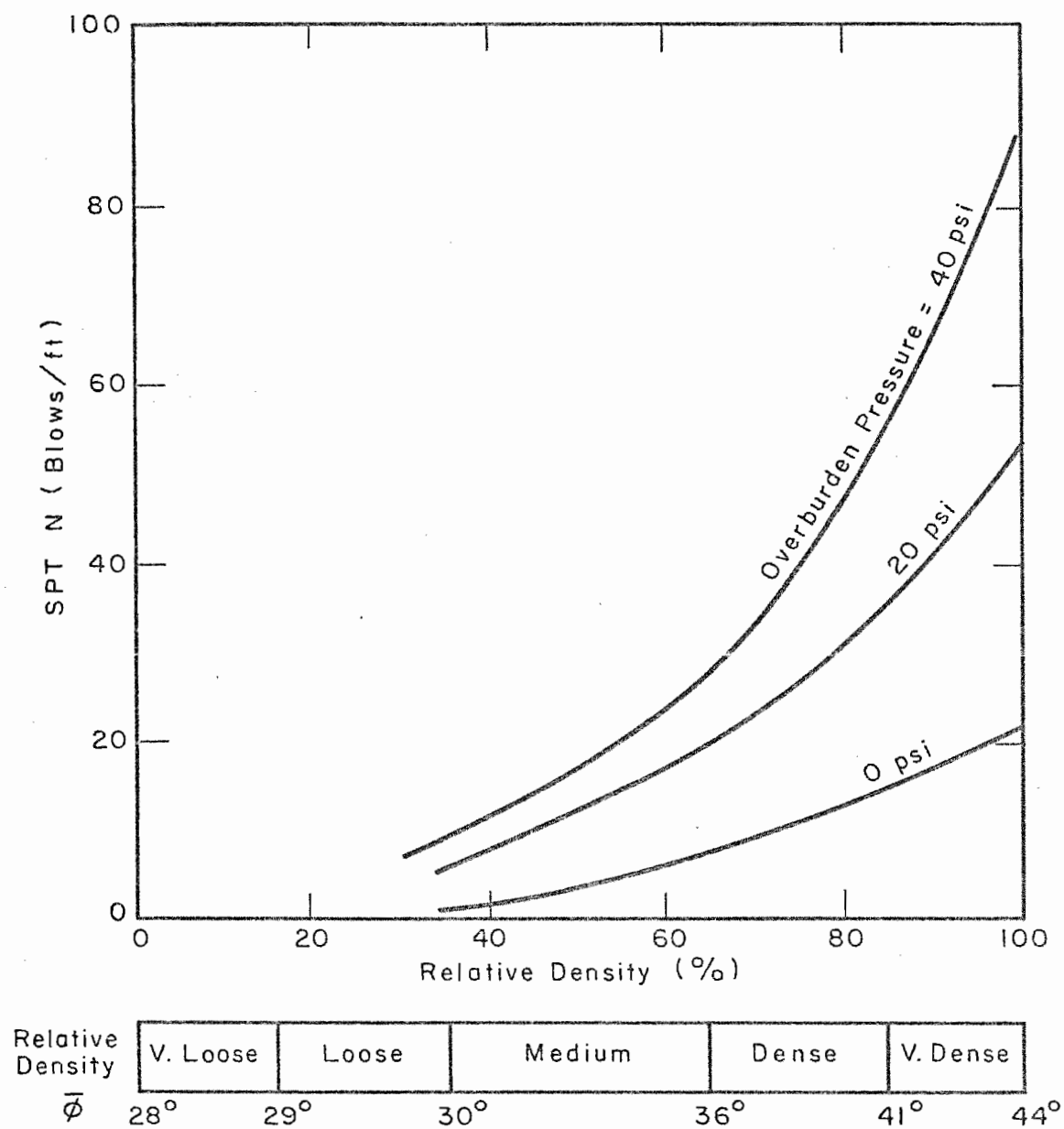


Fig. 4 U.S.B.R. Charts (Gibbs and Holtz)

E. Load Transfer Related to Soil Shear Strength

Previous research has shown that in most soils the load transfer is related to the shear strength of the soil by a constant conventionally called the α factor. In this research, the average α factor (α_{avg}) shall be defined as the ratio of the measured load transferred in a stratum at the failure load (obtained by the double-tangent method) to that predicted by various strength tests. This factor can be evaluated for each shaft as follows:

1. Calculate for each soil layer the predicted unit load transfer by multiplying the layer thickness by the measured shear strength. This expression indicates units of tons per foot of perimeter of the shaft.
2. Using the procedure in Step 1, construct a cumulative diagram of the predicted load transfer for the full entire depth of the shaft (tons per foot of perimeter).
3. Measure the cumulative strength s_c for each stratum by taking from the cumulative diagram the difference between the values at top and bottom of the stratum (tons per foot of perimeter).
4. Compute the predicted load transfer S_p per stratum as:

$$S_p = s_c \cdot C \text{ (tons)}$$

where

C = circumference of shaft.

B. Load-Settlement Curves

The load-settlement curves for each shaft are presented in Figures 6, 10, and 14, as follows:

1. Load-settlement curves for the butt and for the tip from the first test.
2. A load-settlement curve for the butt from each of the subsequent tests.

C. Load-Distribution Curves

Load-distribution curves, Figures 7, 11, and 15, were obtained by plotting the depth of the shaft versus the load measured by the Mustran cells.

This report includes load-distribution curves from the first loading of each shaft as follows:

1. A curve at a load below the ultimate load needed to fail the sides,
2. A curve at the failure load, where the failure load was obtained by the double-tangent method,
3. A curve at the ultimate load applied.

D. Load-Transfer Curves

Load-transfer curves, Figures 8, 12, and 16, were obtained at different depths in the shaft by plotting the shear stress developed at a point versus the displacement of that particular point with respect to its original position. A complete description of the computation procedure followed is explained in full detail in Center for Highway Research Report 89-9.

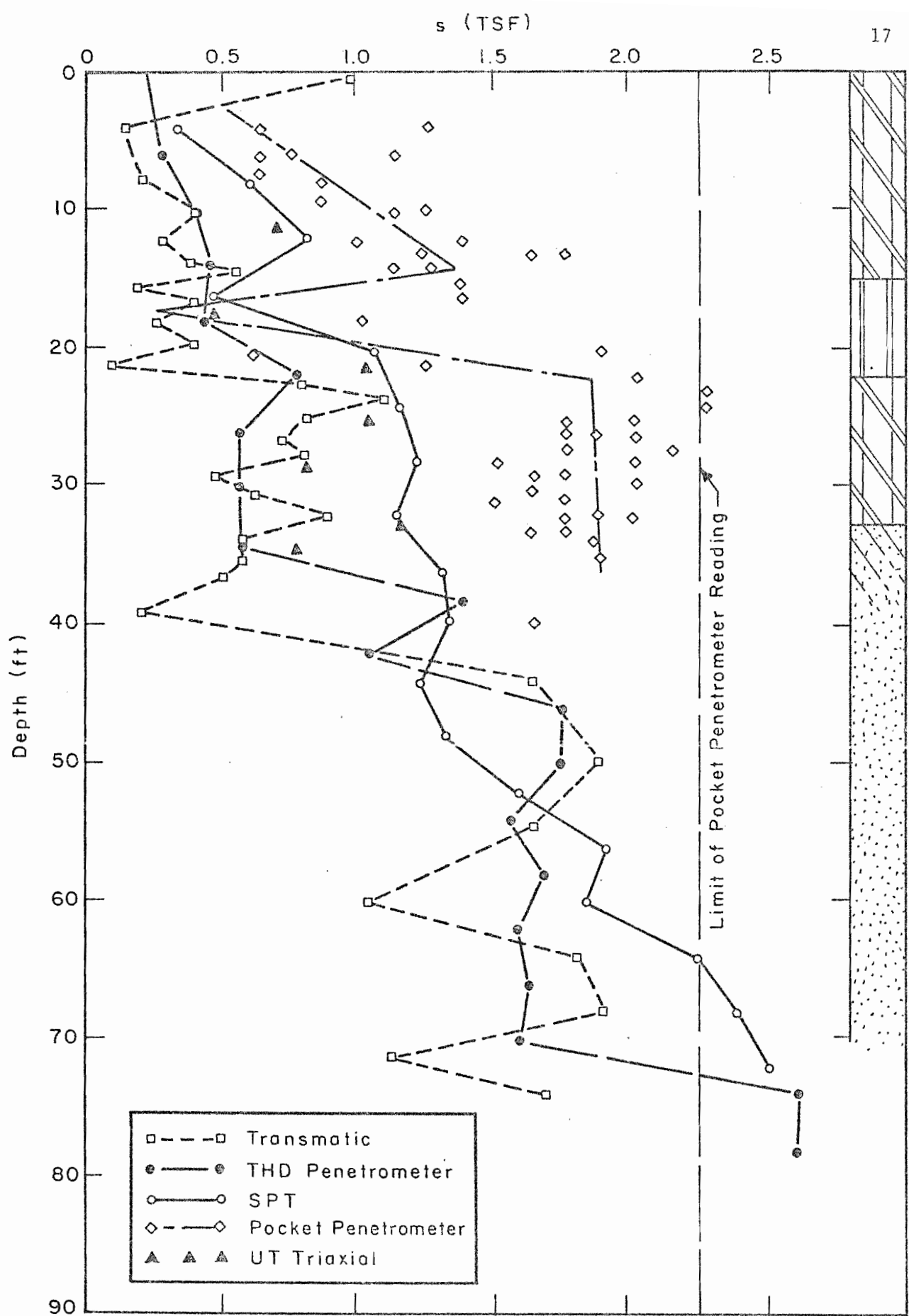


Fig. 5 G1 - Site: Shear Strength Profile

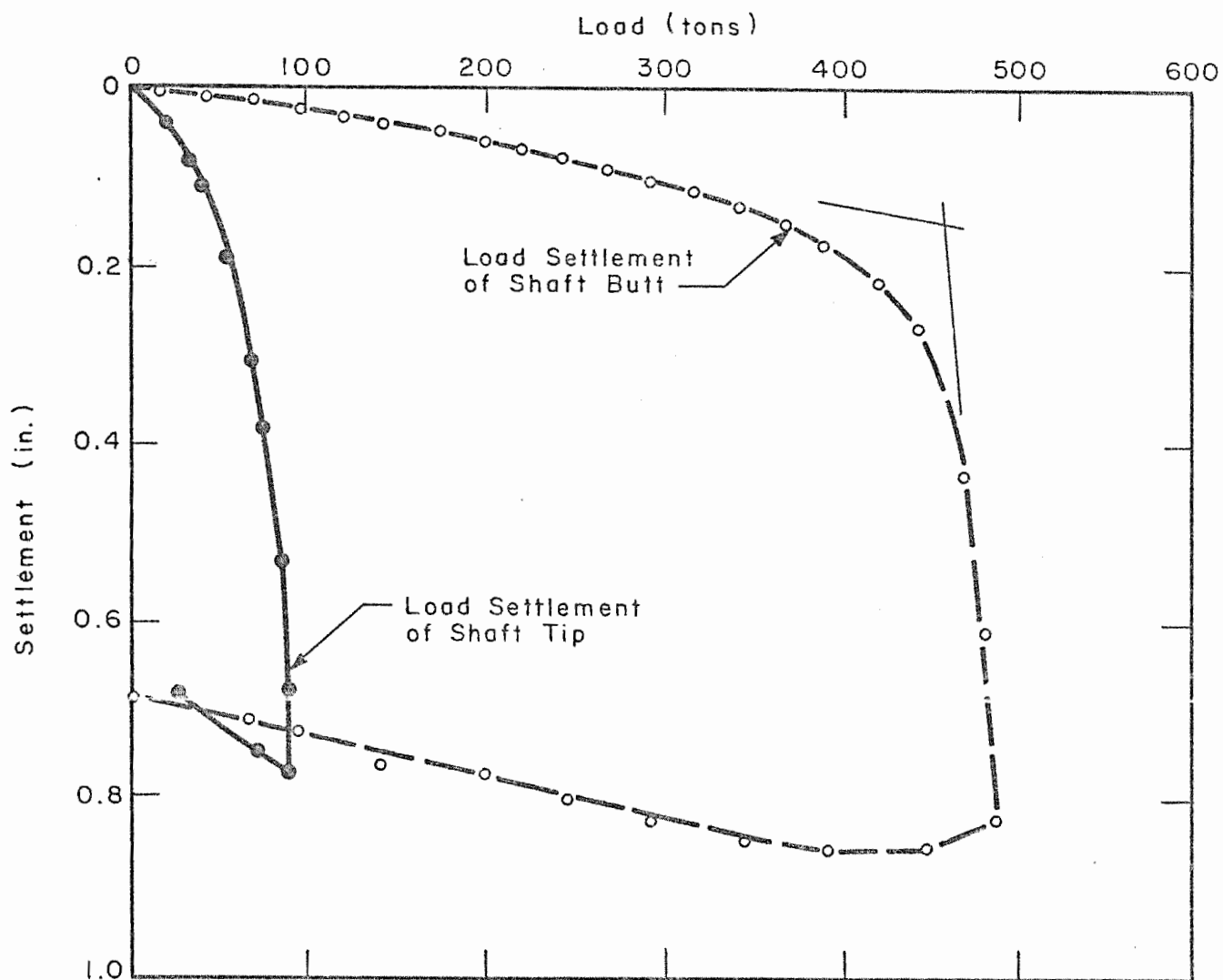


Fig. 6a Load Settlement Curve, G1 - Test 1

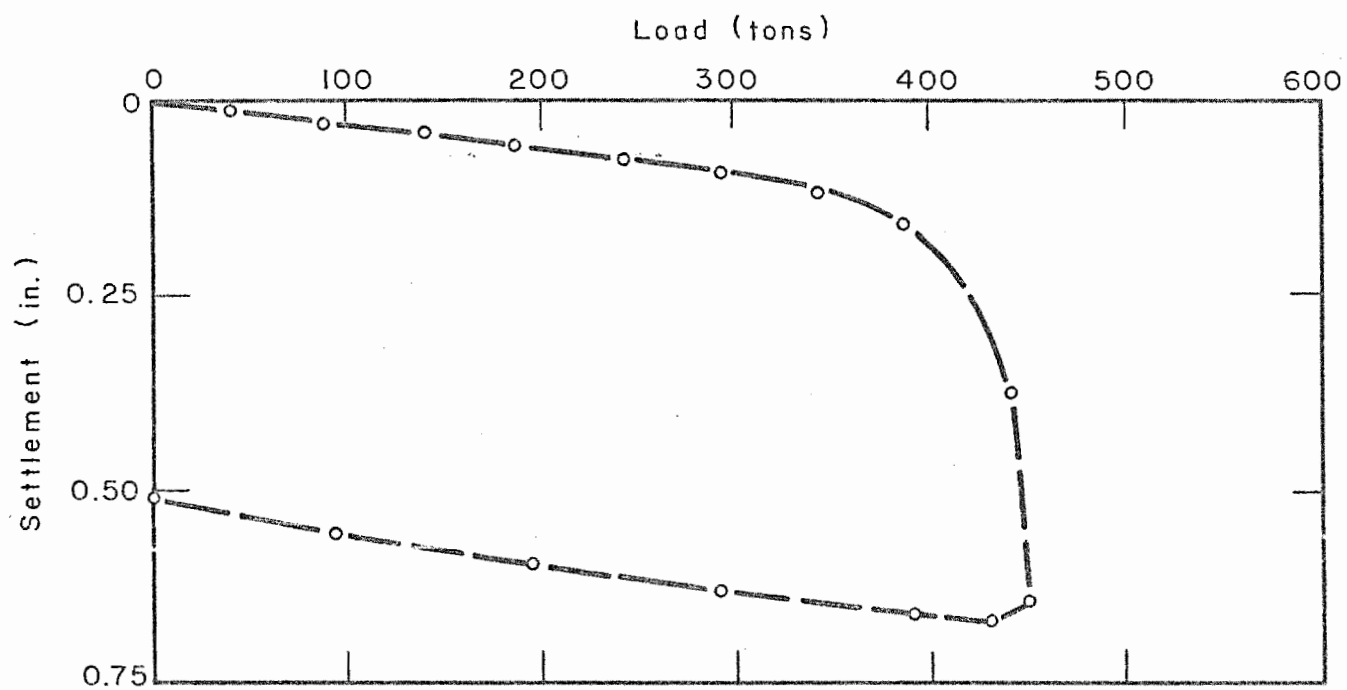


Fig. 6b Load-Settlement Curve, G1 - Test 2

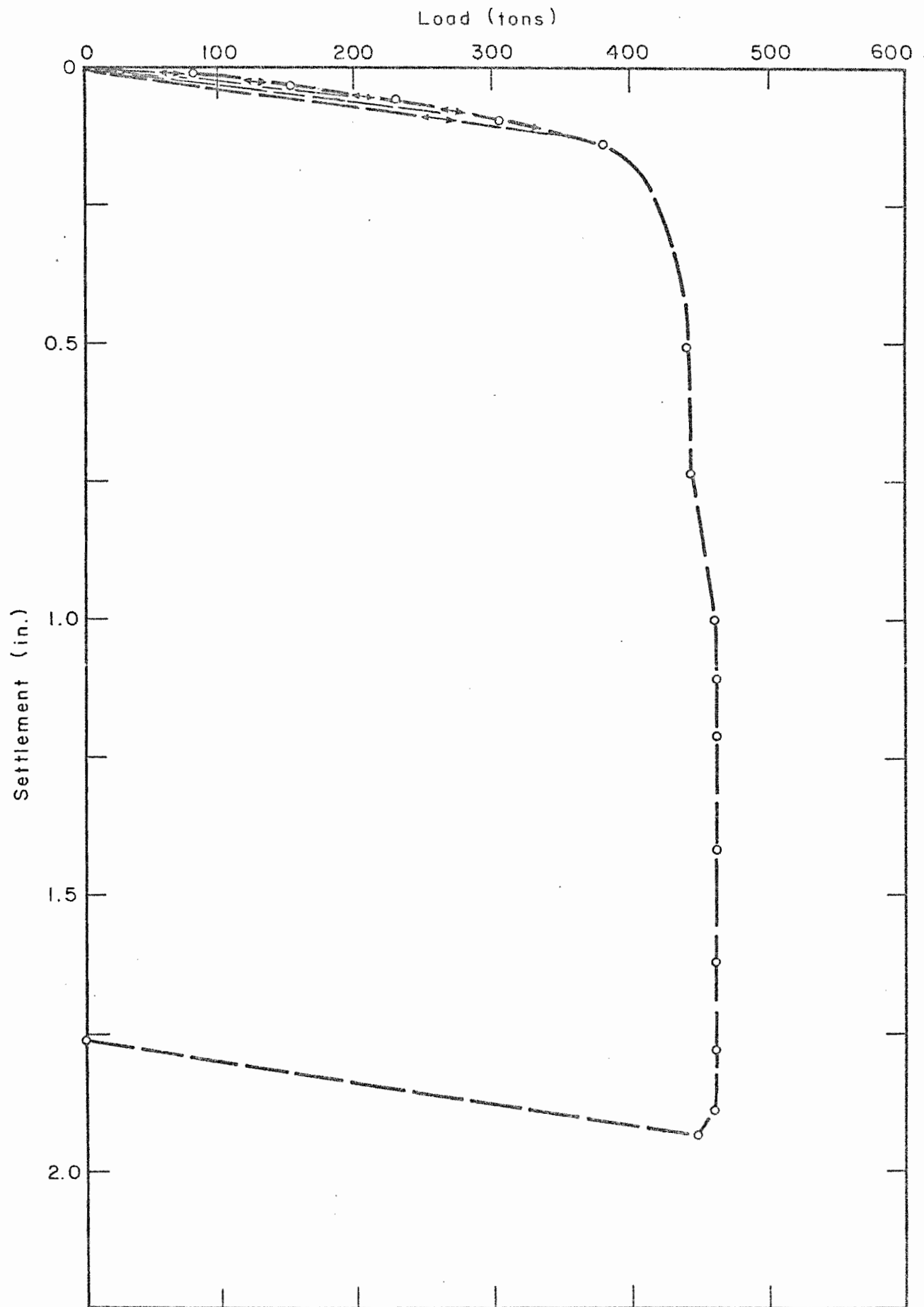


Fig. 6c Load-Settlement Curve, G1 - Test 3

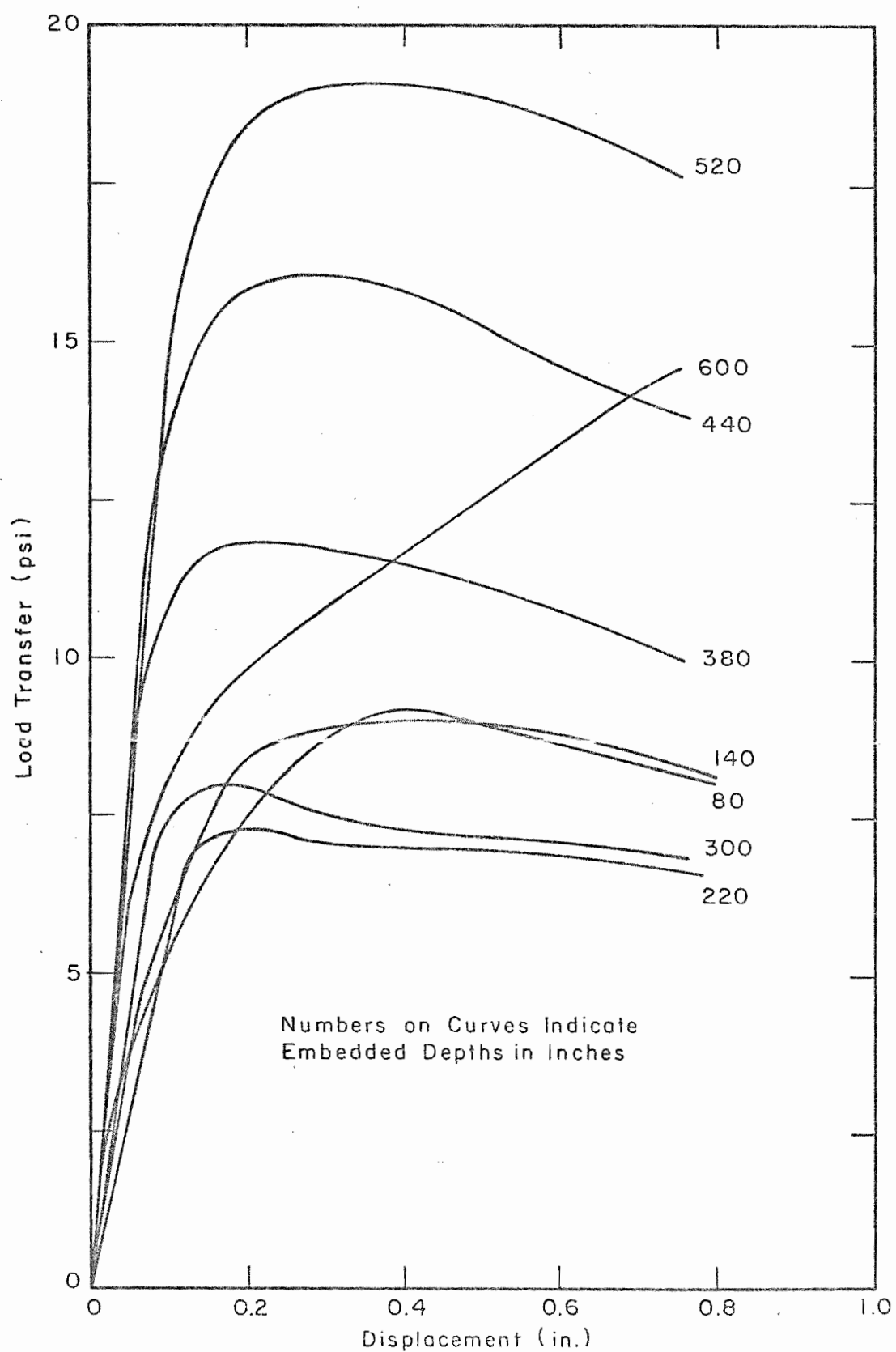


Fig. 8 Load Transfer Curves, G1 - Test 1

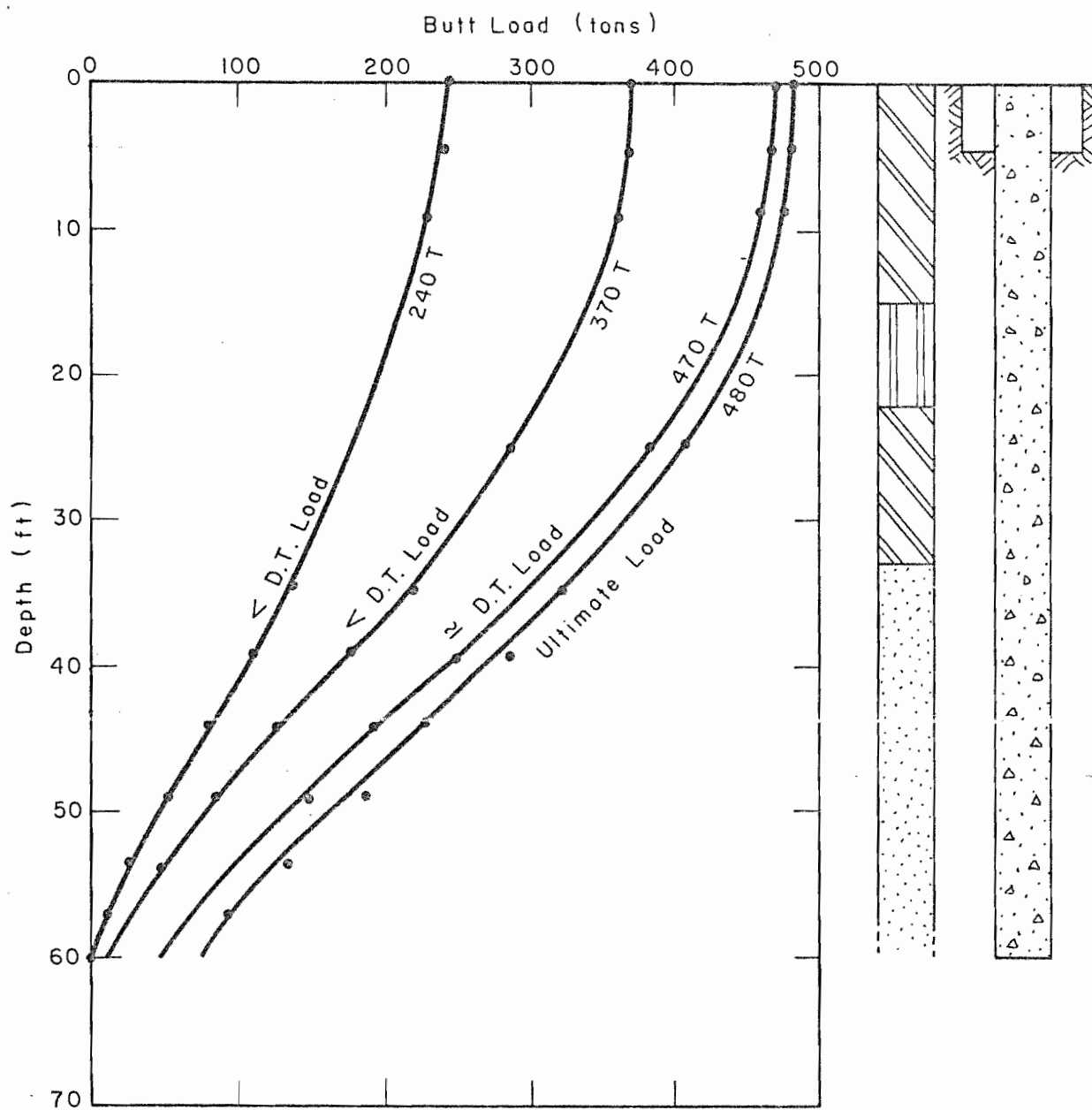


Fig. 7 Load-Distribution Curves, G1 - Test 1

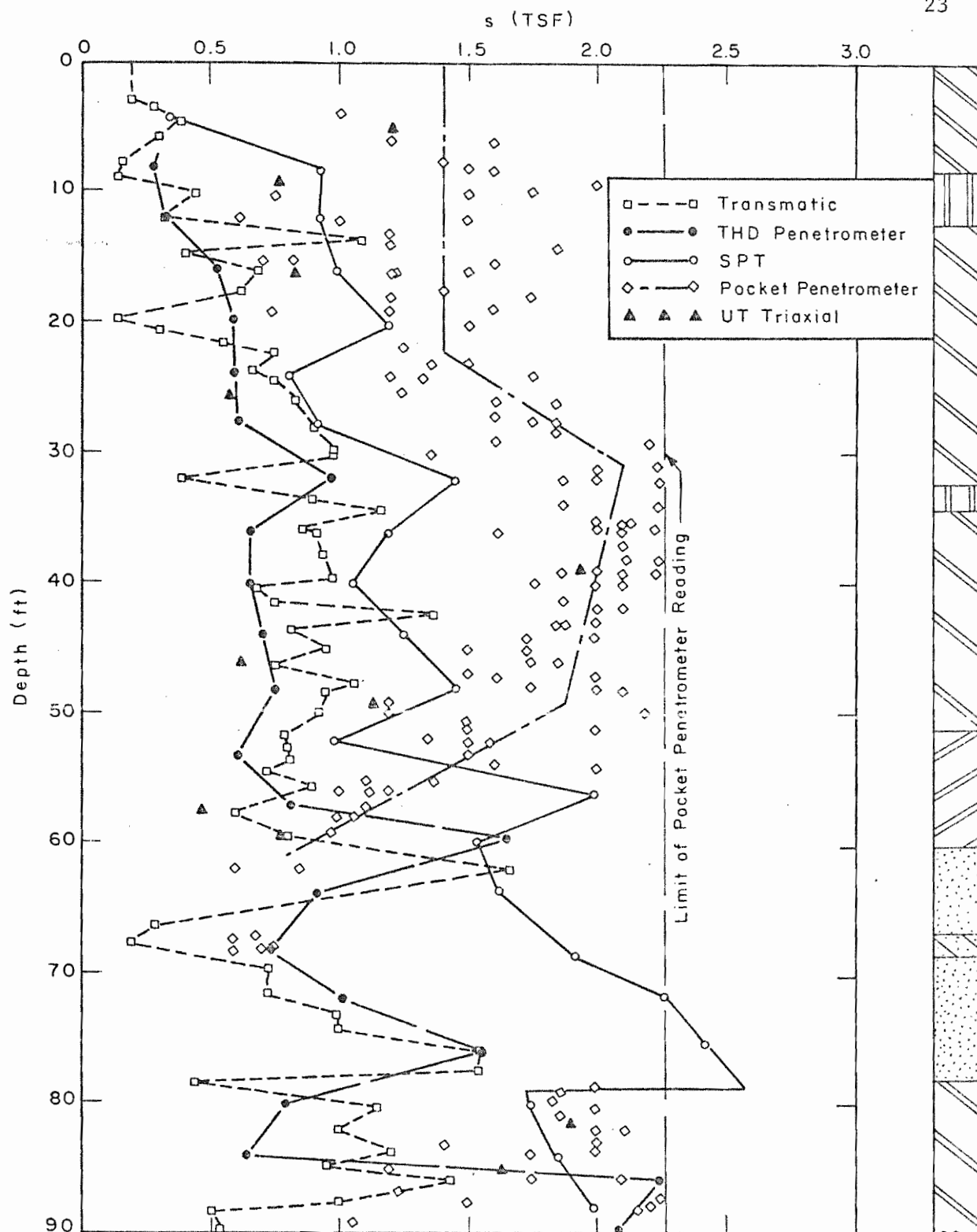


Fig. 9 Shear Strength Profile, G2

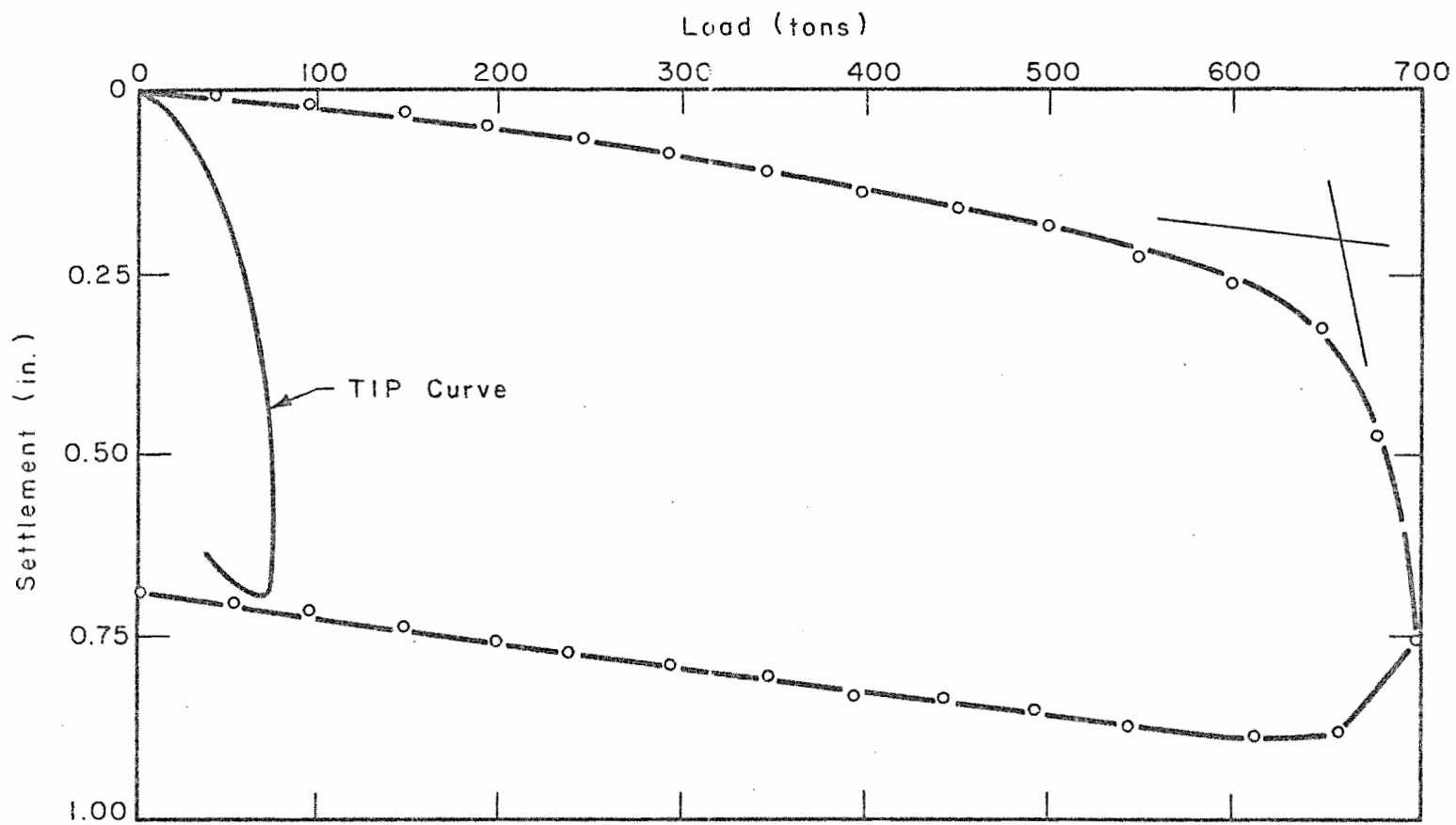


Fig. 10a Load-Settlement Curves, G2 - Test 1

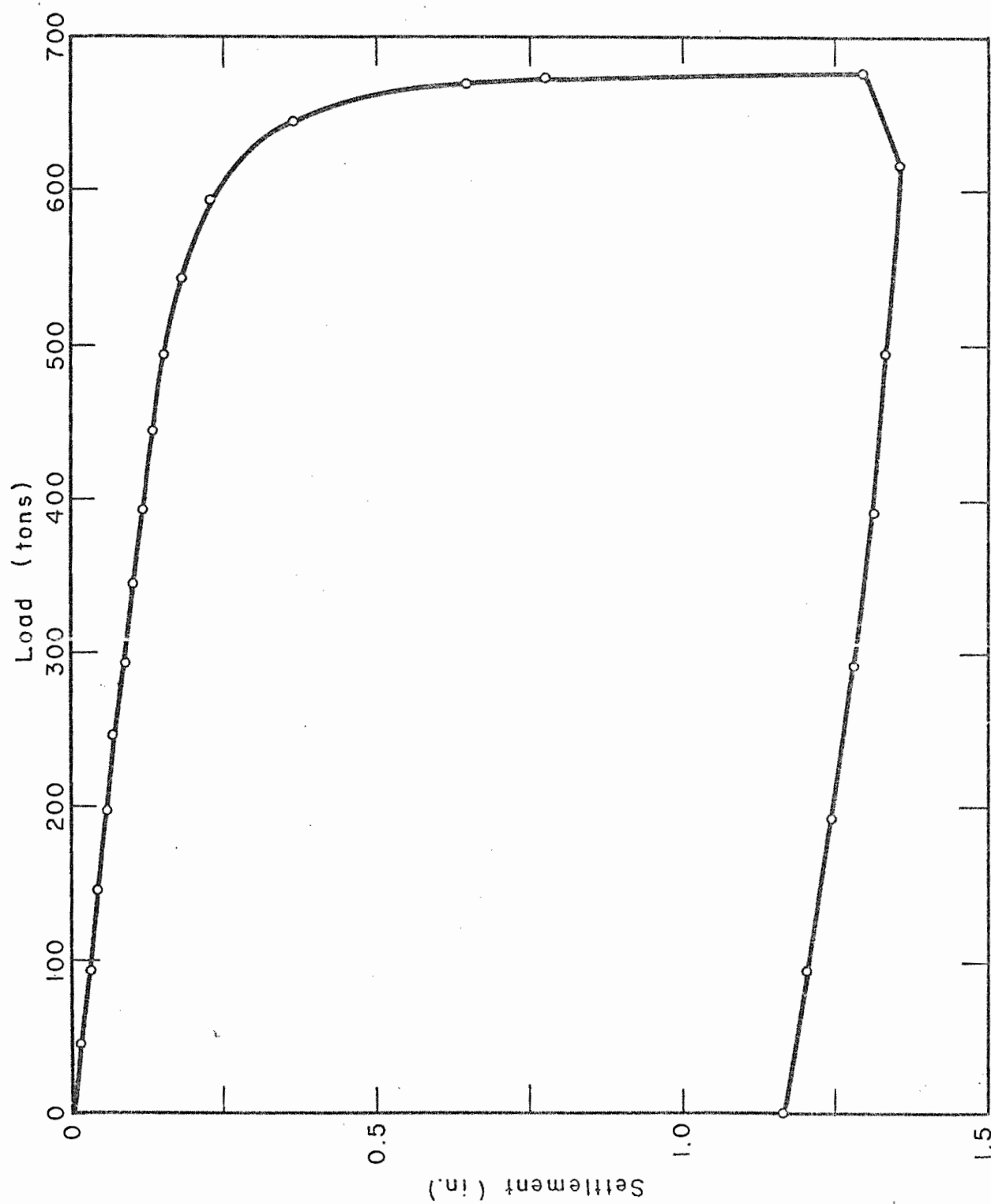


Fig. 10b Load-Settlement Curve, G2 - Test 2

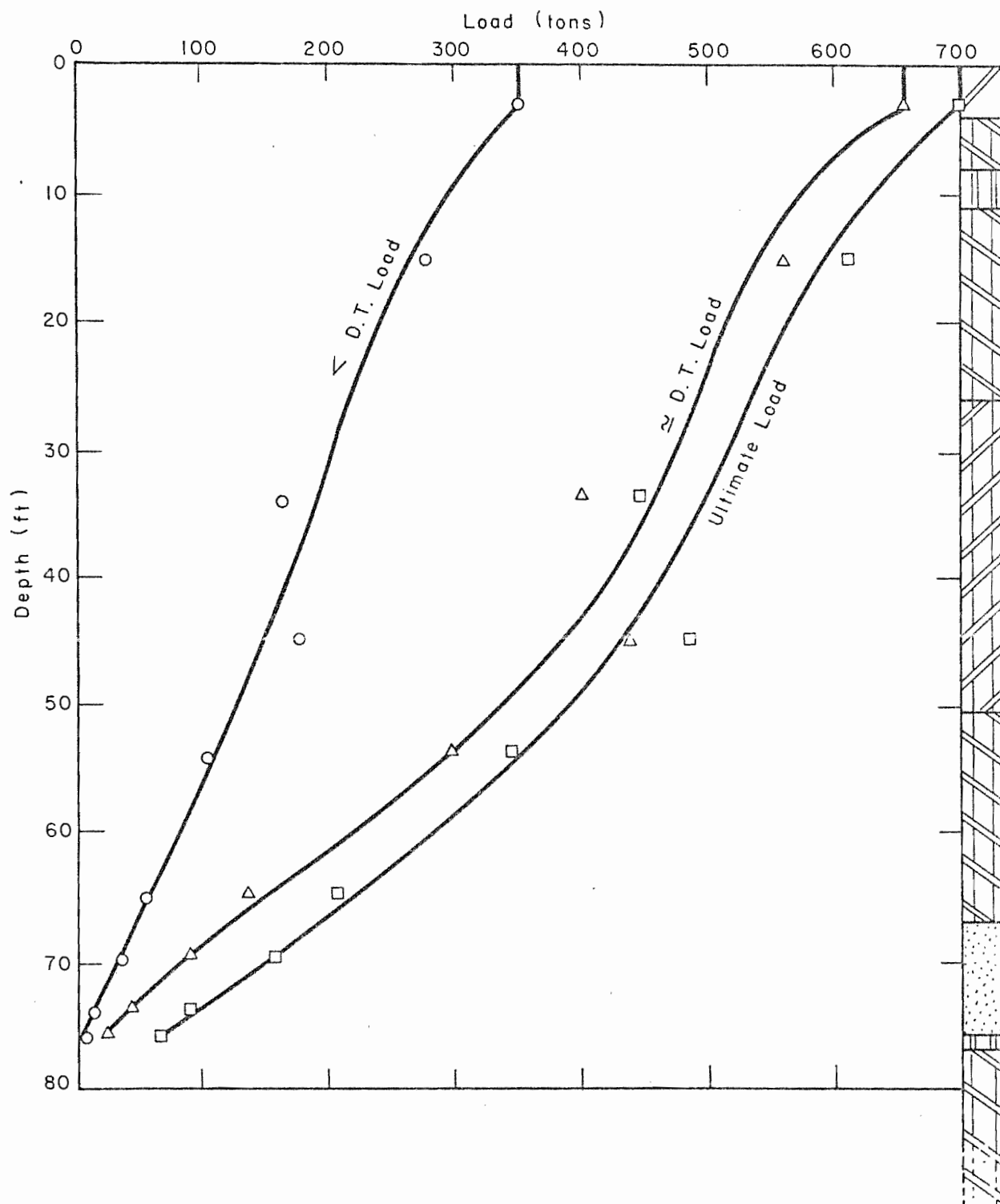


Fig. 11 Load-Distribution Curves, G2 - Test 1

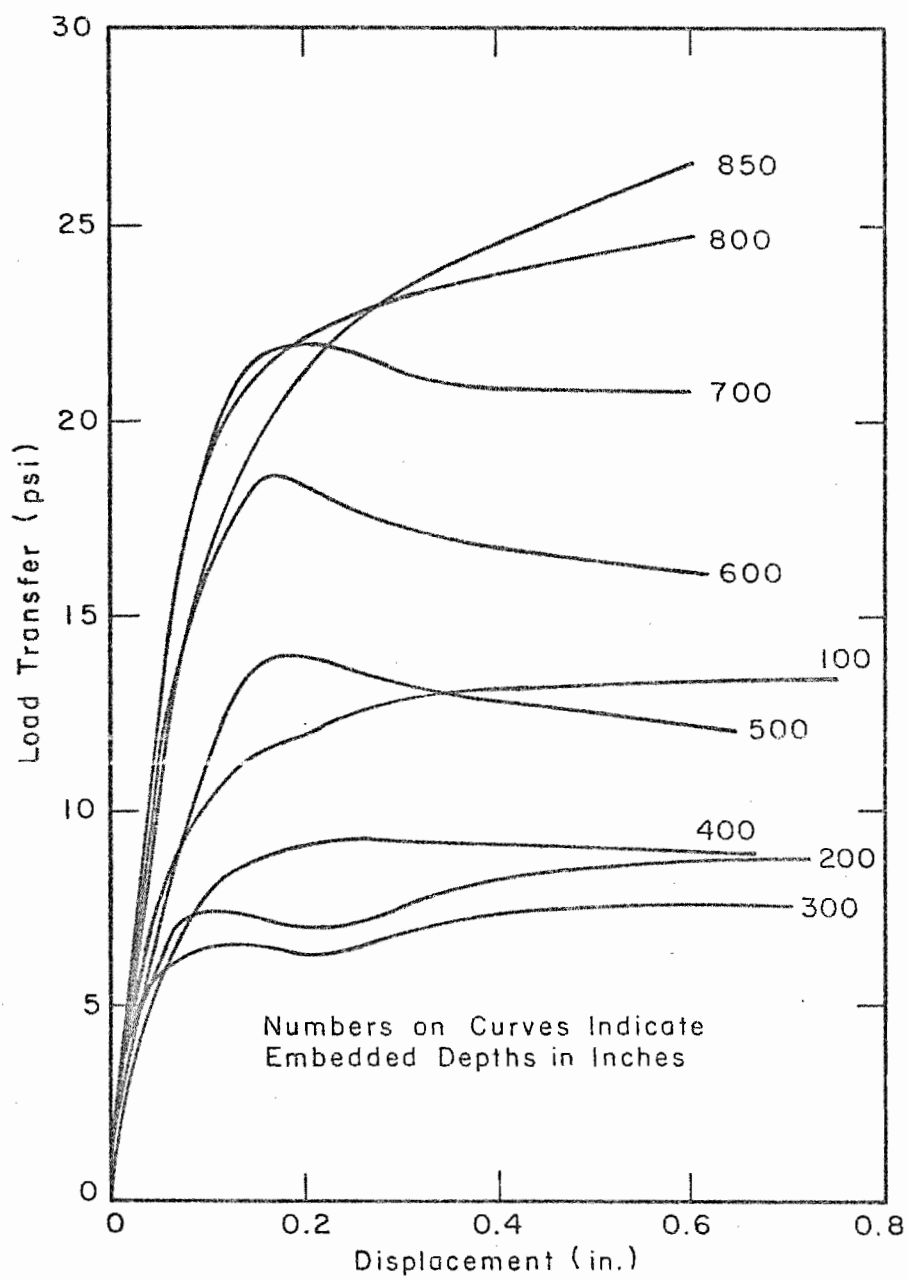


Fig. 12 Load Transfer Curves, G2 - Test 1

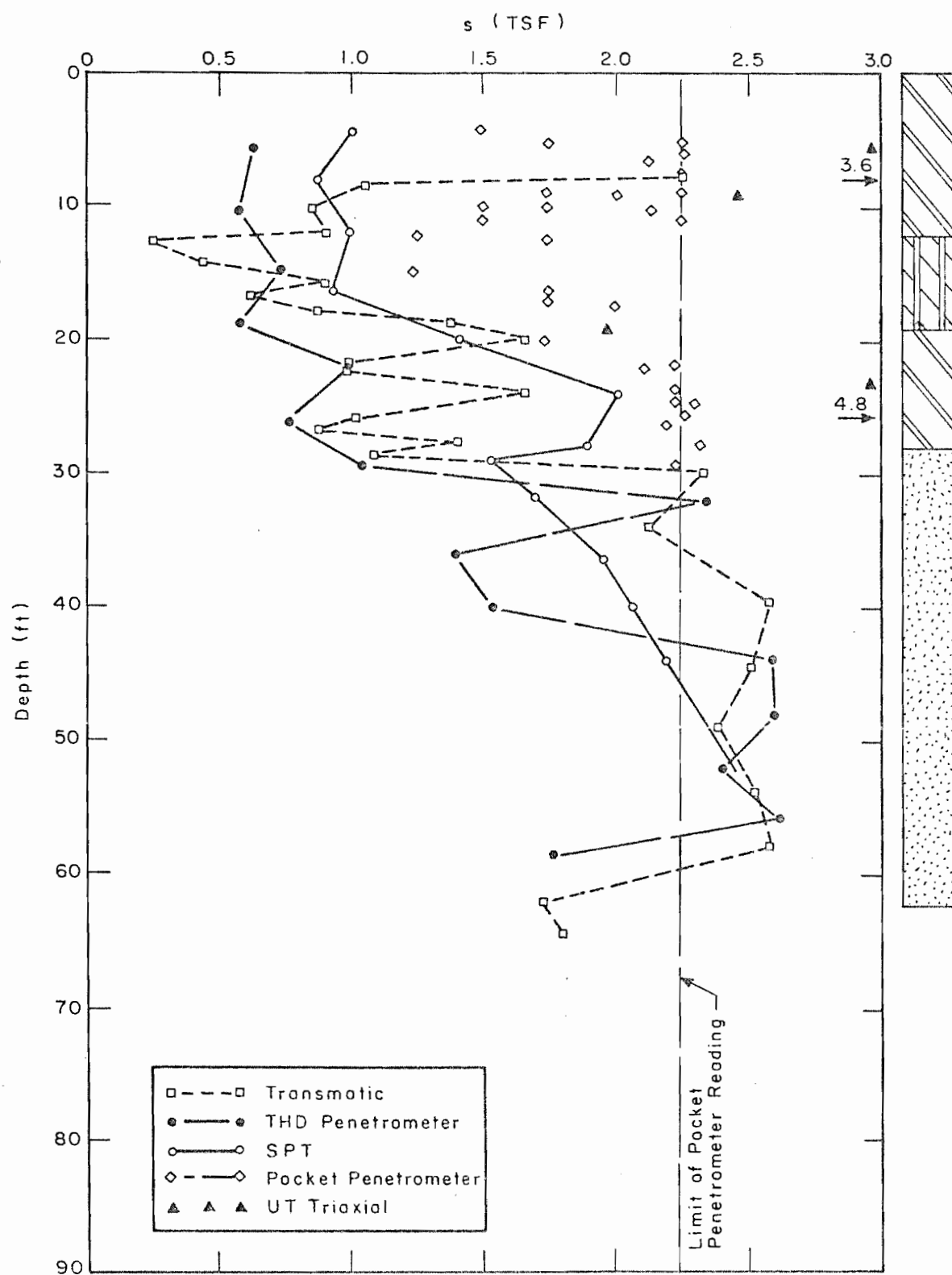


Fig. 13 Shear Strength Profile, BB

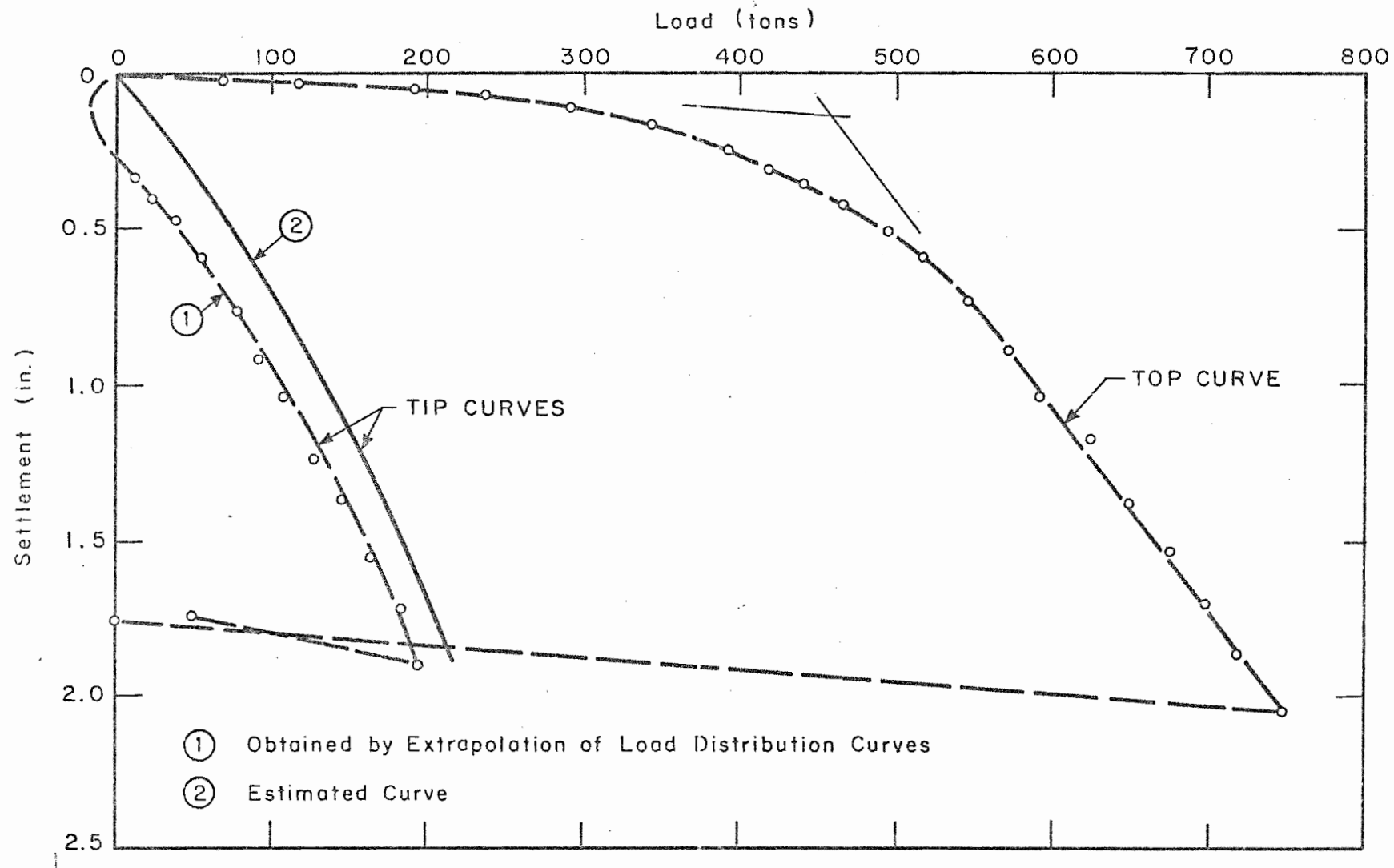


Fig. 14a Load-Settlement Curves, BB - Test 1

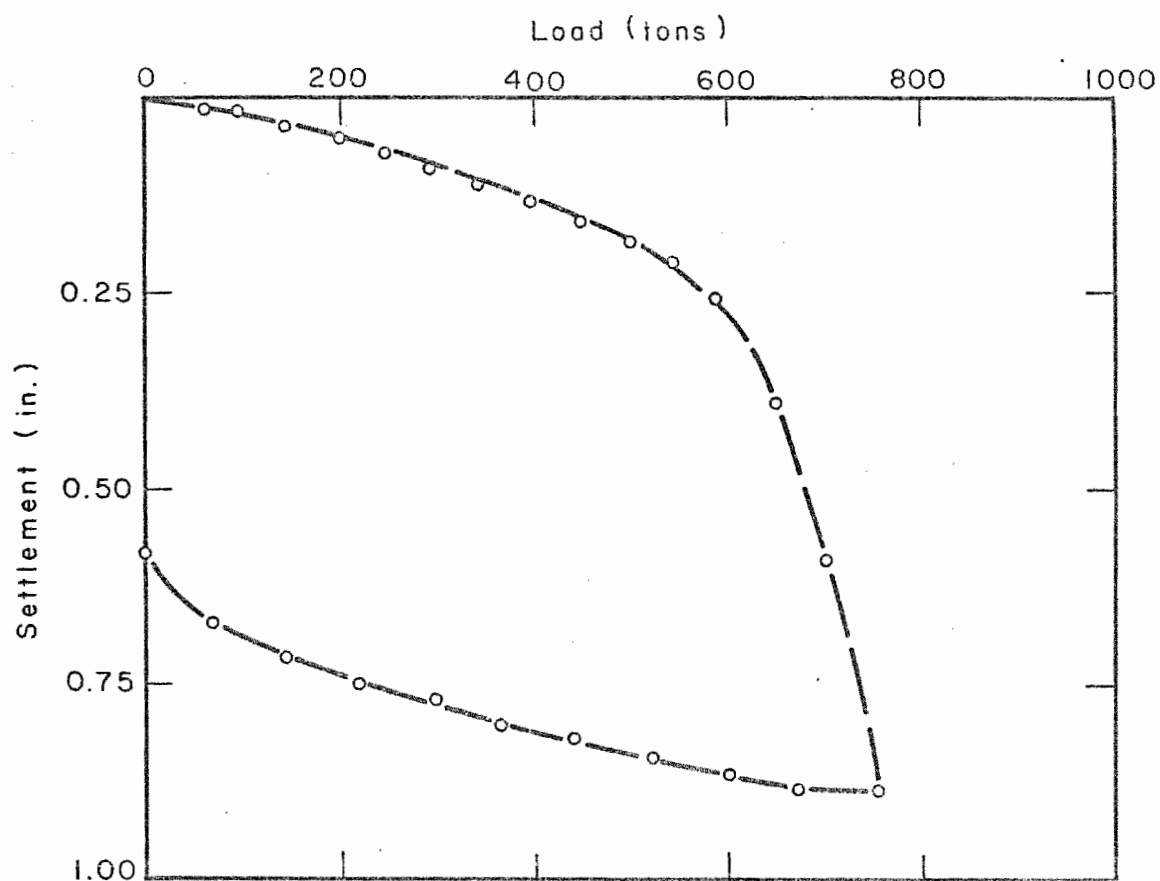


Fig. 14b Load-Settlement Curves, BB - Test 2

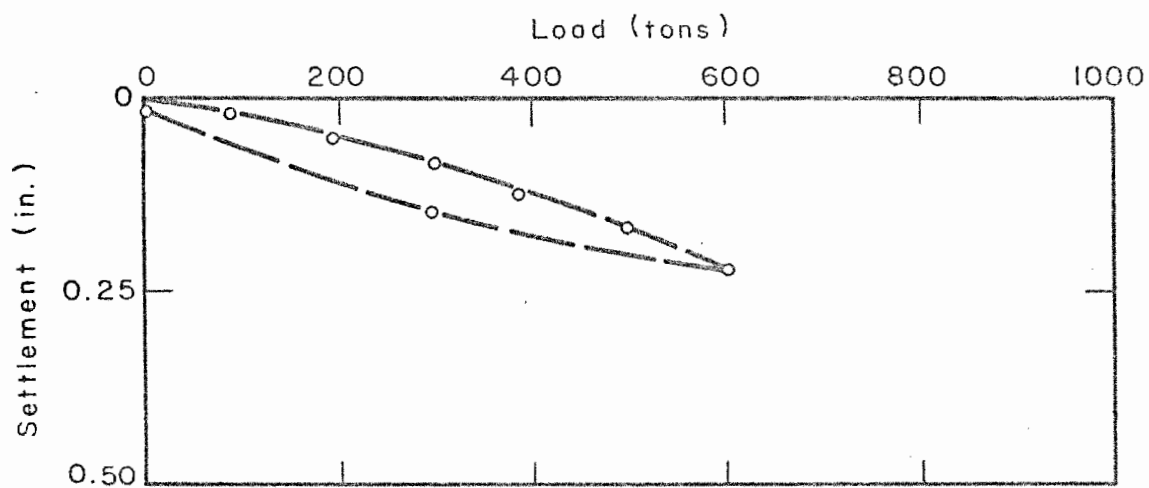


Fig. 14c Load-Settlement Curves, BB - Test 3

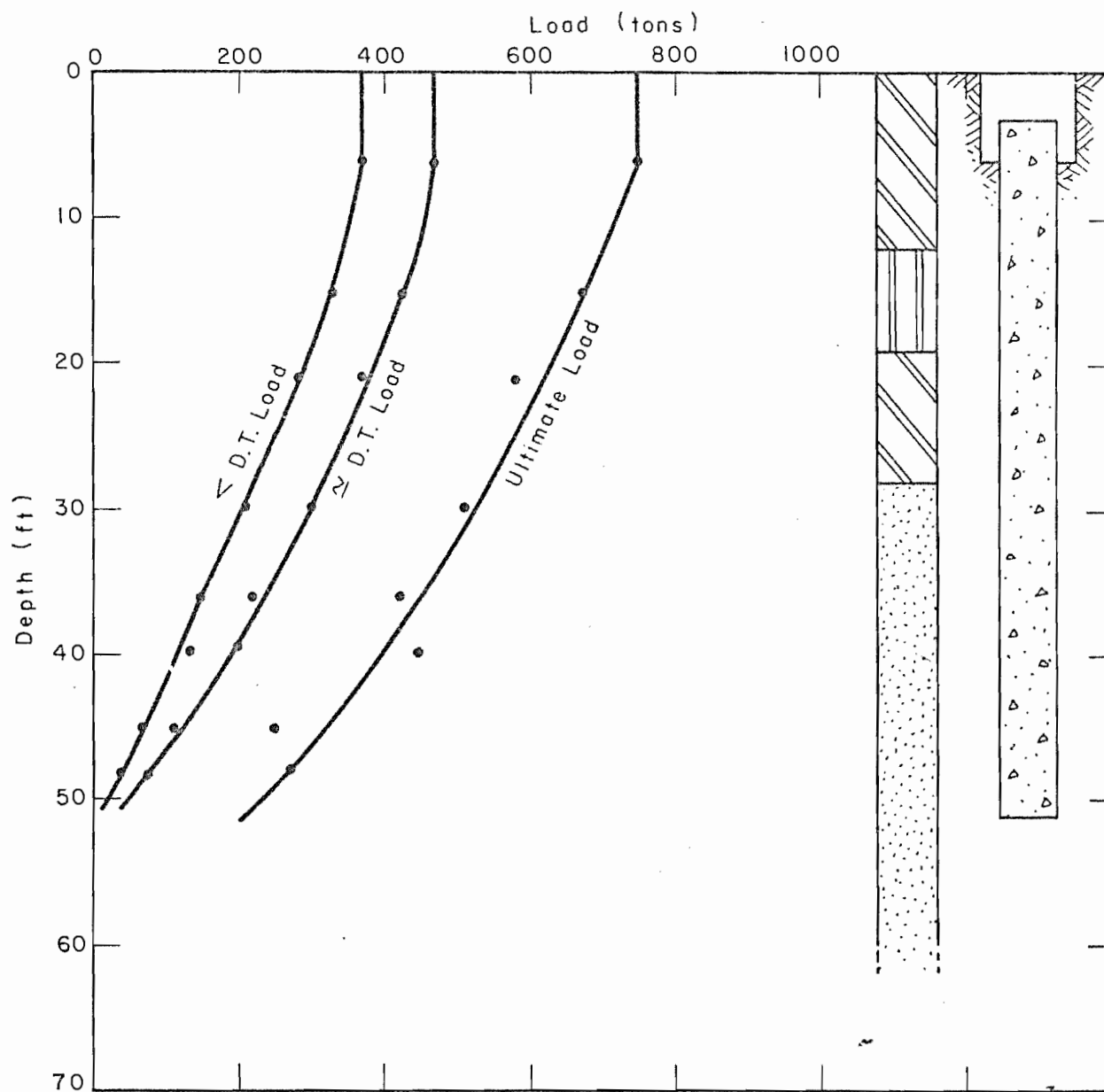


Fig. 15 Load-Distribution Curves, BB - Test 1

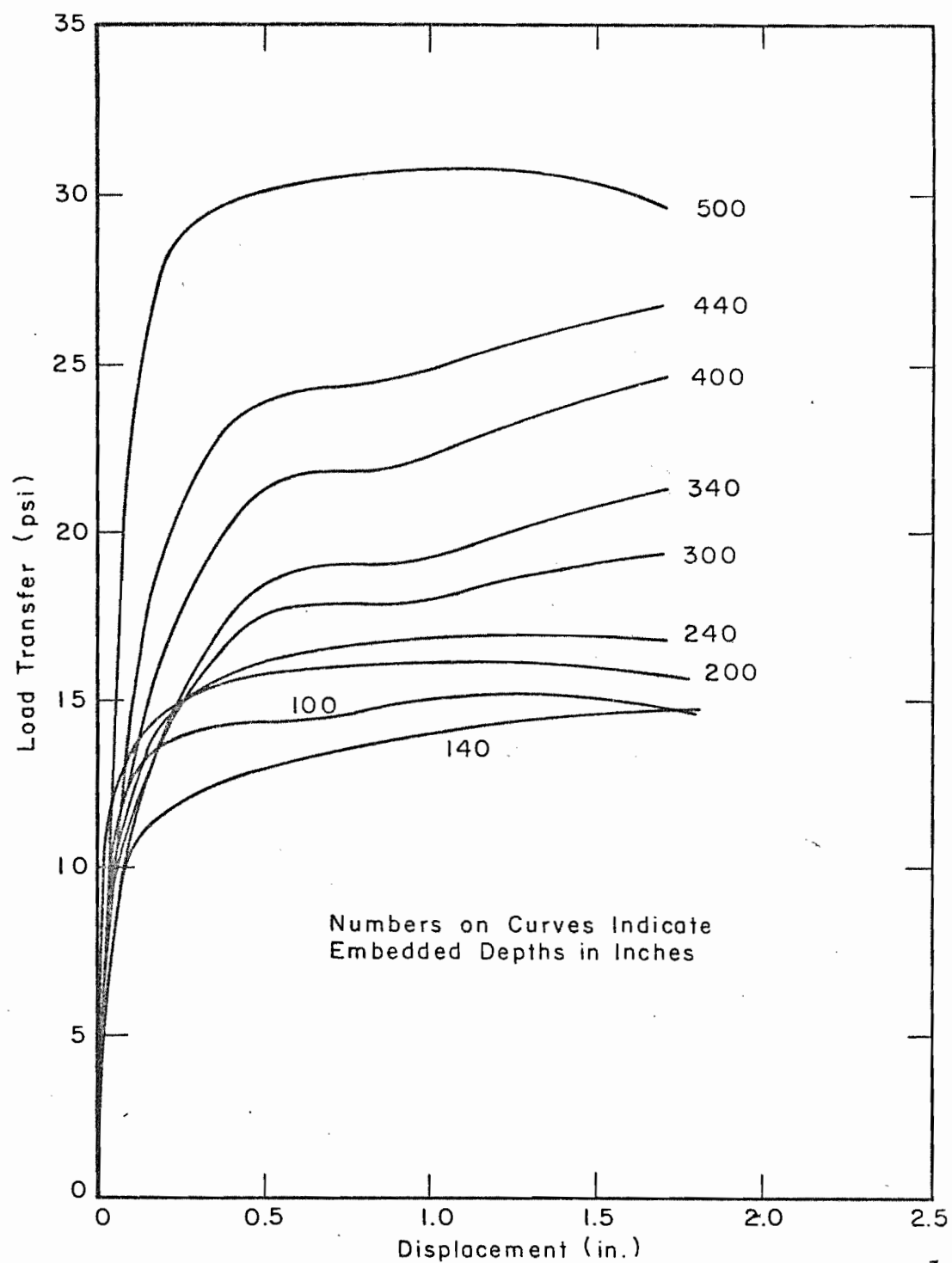


Fig. 16 Load Transfer Curves, BB - Test 1

5. Measure from the load distribution curve at the double tangent load, the load S_m transferred into that stratum (tons).
6. Compute the factor α_{avg} as:

$$\alpha_{avg} = \frac{S_m}{S_p}$$

The cumulative diagrams prepared by the Houston Urban Office (see Appendix) were used to evaluate the α_{avg} factors from the transmatic triaxial and the THD penetrometer test. The values were multiplied by 2 to transform them from safe to ultimate. Similar diagrams to evaluate the α_{avg} factors from the SPT and the pocket penetrometer tests were separately prepared (Appendix II).

Tables 4 through 6 present the α_{avg} factor for each shaft, while Table 7 summarizes these results.

Discussion of Results

A. Shear Strength Profiles

The definition given to the shear strength of sand as obtained from SPT blow count is only a convenient one and is not correct, as it assumes an earth pressure coefficient of 1. Therefore, the effect of the unknown earth pressure coefficient and the adhesion factor between concrete and sand shall be lumped into the α factor.

The pocket penetrometer results indicate a large scatter which is explained by the heterogeneity of the fissured clay. Because the maximum capacity of the instrument used was limited to an unconfined compression strength of 4.5 tsf, higher values could not be measured.

TABLE 4. CORRELATION BETWEEN LOAD TRANSFER
AND SHEAR STRENGTH: G1

Method	Soil	s_c (T/ft)	S_p (T)	S_m (T)	α_{avg}
Transmatic	Clay	6.80	135	145	1.07
THD Penetrometer	Clay	7.00	139	145	1.04
	Sand	20.20	400	280	0.70
Pocket Penetrometer	Clay	34.75	344	145	0.42
SPT	Clay	24.00	236	145	0.62
	Sand	44.00	435	280	0.65

The average maximum unit load transfer as measured is:

in clay = 0.525 tsf

in sand = 1.05 tsf

s_c = Cumulative shear strength per stratum (T/ft, perimeter)

S_p = Predicted load transfer per stratum (Tons)

S_m = Measured load transfer per stratum (Tons)

α_{avg} = Ratio of measured load transfer to predicted load
transfer per stratum

TABLE 5. CORRELATIONS BETWEEN LOAD TRANSFER
AND SHEAR STRENGTH: G2

Method	Soil	s_c (T/ft)	S_p (T)	S_m (T)	α_{avg}
Transmatic	Clay 1	16.5	272	320	1.17
	Clay 2	7.5	123	220	1.78
THD Penetrometer	Clay 1	14.0	230	320	1.39
	Clay 2	7.8	128	220	1.72
	Sand	4.5	74	125	1.69
Pocket Penetrometer	Clay 1	82.9	680	320	0.47
	Clay 2	24.0	197	220	1.12
SPT	Clay 1	51.5	425	320	0.75
	Clay 2	24.0	197	220	1.12
	Sand	22.5	185	125	0.675

The average maximum unit load transfer as measured is:

in clay 1 (overconsolidated fissured Beaumont clay) = 0.81 tsf

in clay 2 (slightly overconsolidated gray clay) = 1.62 tsf

in sand = 1.79 tsf

s_c = Cumulative shear strength per stratum (T/ft, perimeter)

S_p = Predicted load transfer per stratum (Tons)

S_m = Measured load transfer per stratum (Tons)

α_{avg} = Ratio of measured load transfer to predicted load transfer per stratum

TABLE 6. CORRELATIONS BETWEEN LOAD TRANSFER
AND SHEAR STRENGTH: BB

Method	Soil	s_c (T/ft)	S_p (T)	S_m (T)	α_{avg}
Transmatic	Clay	12.0	198	170	0.856
THD Penetrometer	Clay	8.0	132	170	1.290
	Sand	32.0	378	290	0.777
SPT	Clay	30.2	248	170	0.685
	Sand	47.0	387	290	0.750

The average maximum unit load transfer as measured is:

in clay = 0.94 tsf

in sand = 1.53 tsf

s_c = Cumulative shear strength per stratum (T/ft, perimeter)

S_p = Predicted load transfer per stratum (Tons)

S_m = Measured load transfer per stratum (Tons)

α_{avg} = Ratio of measured load transfer to predicted load transfer per stratum

TABLE 7. SUMMARY OF RESULTS ON CORRELATION FACTOR

Shaft	Soil	α_{avg}		SPT
		Triaxial Transmatic	THD Penetrometer	
G1	Clay	1.07	1.04	0.675
	Sand	--	0.70	0.705
G2	Clay 1	1.17	1.39	0.75
	Clay 2	1.78	1.72	1.12
	Sand	--	1.69	0.675
BB	Clay	0.857	1.29	0.685
	Sand	--	0.77	0.75

TABLE 8. MEASURED TIP RESISTANCES AT ULTIMATE LOAD

Shaft	α_{avg}	
	Triaxial Transmatic	THD Penetrometer
G1	90	11.6
G2	80	14.8
BB	220	40.8

The lower layers at the G2 site were very heterogeneous. The soil profile at the shaft location did not agree below 50 feet with the preliminary borings at the site. As observed during construction, and as later concluded from examinations of the soil adhering to the extracted shaft, the soil profile is more like that shown in Fig. 10. This profile indicates a greater depth of the gray clay layer which on the borings showed a pocket penetrometer shear strength varying between 2.0 and 1.0 tsf from top to bottom of the layer. It is believed that a shear strength of 1.5 tsf is a reasonable average for that layer.

B. Load-Settlement Curves

The load-settlement curves for shafts G1 and G2 indicate a sharp drop at ultimate loads which is explained by the lack of tip resistance and by the sensitivity of the clay formation. For shaft BB the load kept building up even at high displacements, which is a characteristic of drilled shafts with tips in sand.

Table 8 summarizes the results of the tip resistance. The ultimate pressures at G1 and G2 were reached only at large settlements. At settlements corresponding to failure load obtained by the double-tangent method, the tip pressures were only about half of the ultimate tip resistance.

Shaft BB developed a considerable tip resistance which is explained by the fact that there appeared to be less soft deposits at the bottom of the hole. In the other cases (shafts G1 and G2) the bottom sediments contained soft material, and the tip resistances were relatively small.

C. Load-Distribution Curves

The load-distribution curves were obtained from data from the Mustran cells which were embedded in the shafts. Some cells did not register

the correct load in the concrete due to entrapped mud at the end caps, a fact physically proved when some of the suspected cells were exposed. Cells on shafts G1 and G2 had less entrapped mud than those at shaft BB because the mud at this latter site was unusually thick and did not allow a good concrete flow. Readings from cells that showed any evidence of trapped mud were discarded.

The Young's modulus as measured on concrete cylinders indicated a considerable scatter (about 20 percent). This fact plus the fact that concrete from three different trucks was used in casting the G2 shaft may account for the large scatter in data at this shaft.

The cells at the calibration level at shaft BB showed evidence of trapped mud; therefore, data from these cells were discarded. A calibration curve was estimated from knowledge of the behavior of similar cells in similar concrete and was used in reducing the data. The lack of a good set of load cells at the calibration level added some uncertainty to the validity of the results from load cells at this shaft.

D. Load-Transfer Curves

The general observation can be made that the ultimate load transfer in Beaumont clays is reached for relative movement between the shaft and the soil of 0.15 to 0.2 in., while for sands this relative movement varied between 0.2 in. for shaft G1 to 0.5 in. for shaft BB. The reasons for this wide range of displacements at failure in sands is not yet well understood.

E. Load Transfer Related to Shear Strength

The load transfer in sands as measured in shafts BB and G1 indicate an α_{avg} factor of about 0.7 with respect to that calculated from THD

cone penetrometer data. This value is understood to be valid for:

1. Shafts constructed by the direct slurry displacement method,
2. An embedment in sand of about 20 to 30 feet,
3. Failure loads obtained by the double-tangent method.

The α_{avg} factor evaluated for the THD cone penetrometer in the sand at the G2 site does not agree with values obtained from the other test sites. This difference can possibly be explained in terms of the following factors:

1. The dynamic penetrometer test, when used in clayey sands or in sands interbedded with layers of clay, tends to show smaller resistance to penetration due to lubrication by the clay and due to undissipated pore pressures created by the quick impact.
2. The resistance to penetration of a dynamic penetrometer is also a function of depth. In general, at greater depths the increased weight of the stem results in an easier penetration.
3. The procedure followed to evaluate the shear strength of sands from the blow count of the THD cone penetrometer may not be correct, and it is believed that a procedure like that followed to evaluate shear strength from the standard penetration test is more rational.

Table 9 shows tabulations of α_{avg} obtained from results of previous load tests on drilled shafts in Beaumont clay which were cast by using the dry method (O'Neill and Reese, 1970). As can be seen from studying

TABLE 9. CORRELATION FACTORS FROM PREVIOUS RESEARCH

Test	Measured average peak load transfer tsf	Transmatic Triaxial		THD Penetrometer		UT Triaxial	
		Average Shear Strength	α_{avg}	Average Shear Strength	α_{avg}	Average Shear Strength	α_{avg}
S1T1	0.50	0.67	0.74	0.50	1.00	1.25	.44
S2T1	0.60	1.60	1.00	0.45	1.33	1.10	.54
S3T1	0.63	0.67	0.93	0.50	1.26	1.15	.54

the values in the table, the α factor from the tests where the slurry displacement method was used are as high or perhaps higher than those from tests where the dry casting method was used.

The smaller α_{avg} values measured in the very stiff clays at the BB test site are explained by the fact that a shear failure apparently took place at the concrete-soil interface rather than in the soil, as was the case with the other test shafts. It is believed that this result is not due to an early age testing (sixteen days after installation) but rather due to the type of clay being tested.

General Field Observations

A. Drilling Slurry

The average densities of the mud slurry used at each of the sites, obtained by averaging the densities of samples taken from different depths in the hole, are as follows:

G1: 1.3 T/m^3 - 81.0 pcf

G2: 1.052 T/m^3 - 65.6 pcf

BB: 1.4 T/m^3 - 87.5 pcf

The greater content of sands at the G1 and BB sites charged the mud slurry with a considerable amount of sand and, therefore, significantly increased its density, a phenomenon that did not take place in the G2 shaft where the thickness of the sand stratum was only a small portion of the total hole depth.

B. Construction

It appears that the main disadvantage to the slurry displacement method of construction is the development of relatively smaller tip resistance as compared to what would be expected from drilled shafts tipping in sandy

soils. The deposition of loose sediments at the bottom of the hole can create a weak layer of material at the tip of a shaft, resulting in reduced bearing capacity of the tip. These sediments could be the result of the sloughing of walls of the hole, the deposition of soils suspended in the mud, or the entrainment in the hole of loose soil from the ground surface. A rich, well-dispersed mud slurry, maintained near the ground surface, should reduce the amount of sloughing and sedimentation of soils in suspension. After the bottom of the hole has been cleaned, the hole should be protected at the surface by a short piece of casing to prevent loose surface soil from falling in the hole.

Cleaning of the bottom of the hole should be given serious attention. It was observed that the drilling bucket cleaned the bottom of the hole better than the auger.

The flow of the concrete is mainly affected by the size of the drilled hole, the size of the tremie, the density of the mud slurry, the shear strength of the concrete and its viscosity, the roughness of the tremie and the roughness of the surface of the drilled hole. A vigorous scour by the wet concrete of the walls of the drilled hole is desirable in order to prevent mud entrapment. An analytical description of the flow conditions is a complex problem. However, such an analytical description is necessary before the construction procedure can be optimized. As an example of the kind of problem to be solved, the contractor's representatives suggested on the basis of their experience that a 12-inch tremie would have been better than the 10-inch tremie which was actually employed and was required by the existence of load cells mounted on the steel cage. A valid analytical procedure for the flow problem could allow such questions to be solved rationally.

The first flow of concrete may be used advantageously to clean the bottom of the hole. However, the appearance of the tip of the extracted shafts suggested that the polyethylene sheet used to seal the end of the tremie, as it was first lowered, probably prevented an effective washing action of the first flow of the wet concrete. The size of the polyethylene sheet should be minimized or preferably a better sealing technique should be devised.

C. Concrete and Concrete-Soil Interface

In the BB and G1 shafts, it was observed that small amounts of mud slurry were trapped in the concrete. The slurry was observed mainly in the upper portion of the shaft and on instrumentation cables, gages, and spirals, which provided obstructions to the vertical flow of the concrete. This sort of contamination was minimal in the G2 shaft, probably because the slurry at that shaft was much thinner than at the other two sites. Very little contamination was observed on the vertical bars. The existence of the horizontal obstructions and the decreased hydraulic gradient on the concrete column during the last few feet of flow were the main reasons that the mud slurry was entrapped mainly in the top portion of the shafts.

When a hole is brought to final depth in a formation consisting of sand and clay layers, the walls of the hole are coated with a thin layer of mud and sand. The characteristics of the coating depend on the bentonite which is added to form the slurry and on the sand which is mixed with the slurry as the hole is augered. Depending on the grain-size distribution of the sand formation and the hydrostatic head of the slurry, the cake may penetrate the sand a considerable distance. As the auger is raised

and lowered in the hole, some of the cake from the slurry is deposited on the walls of the hole through the clay strata.

This coating was observed at almost all levels on the extracted shafts. Field examination of the concrete-soil interface indicated in most soil strata a failure surface in the soil rather than at the interface, which means that the coating has a higher shear strength than the surrounding soil. There is a possibility that some stabilization of the cake may take place by chemical reaction with the concrete.

At the BB site, no failure surface was observed in the very stiff clay, and there was evidence of failure taking place right at the interface. The measured shear transfer of about .94 tsf in that clay formation is an indication of the strength of the coating at that level. It is believed that there is a cohesive component and a frictional component of the shear strength of the coating. Thus, at lower depths higher values of shear transfer than those measured at relatively shallow depths may be possible.

REFERENCES

1. Barker, W. R. and Reese, L. C. (1969), Instrumentation for Measurement of Axial Load in Drilled Shafts, Research Report 89-6, Center for Highway Research, The University of Texas at Austin, Texas, 1969.
2. Barker, W. R. and Reese, L. C. (1970), Load-Carrying Characteristics of Drilled Shafts Constructed with the Aid of Drilling Fluids, Research Report 89-9, Center for Highway Research, The University of Texas at Austin, Texas, 1970.
3. Gibbs, H. J. and Holtz, W. G. (1957), "Research on Determining the Density of Sands by Spoon Penetration Testing," Proceedings of the Fourth International Conference of Soil Mechanics and Foundation Engineering, Vol. I, Butterworths, London, 1957.
4. O'Neill, M. W. and Reese, L. C. (1970), Behavior of Axially Loaded Drilled Shafts in Beaumont Clay, Research Report 89-8, Center for Highway Research, The University of Texas at Austin, Texas, 1970.
5. Terzaghi, Karl and Peck, Ralph (1948), Soil Mechanics in Engineering Practice, Wiley, New York, 1948.
6. Texas Highway Department (1964), Foundation Exploration and Design Manual, Bridge Division, Austin, Texas, 1964.

APPENDIX I
BORING LOGS

DATE: 5-27-71
SPT Boring Log
Hole G1-1

Depth, ft.	Blows		
	6" seating	1st 6"	2nd 6"
4	2	2	3
8	2	4	5
12	3	5	6
16	3	4	3
20	5	7	9
24	5	8	9
28	6	8	10
32	4	8	9
36	8	15	16
40	10	14	11
44	7	6	6
48	6	7	7
52	7	10	13
56	8	12	19
60	5	8	16
64	5	21	32
68	8	30	47
72	18	27	34
76	19	20	23

DATE: 5-17-71
SPT Boring Log
Hole G2-1

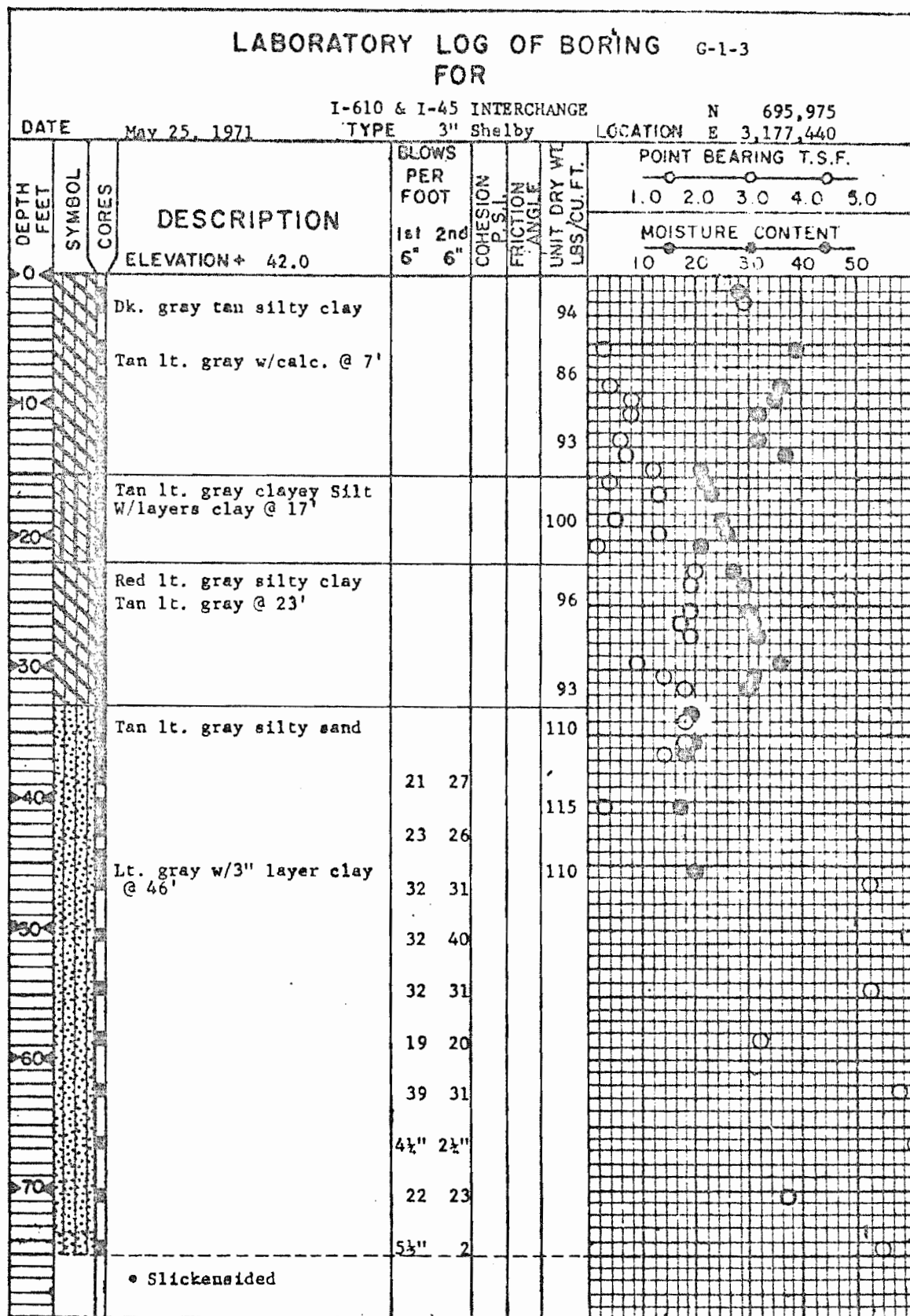
Depth, ft.	Blows		
	6" seating	1st 6"	2nd 6"
4		2	3
8	4	7	7
12	3	6	8
16	4	7	8
20	4	10	8
24	3	5	7
28	3	6	8
32	6	11	11
36	6	9	12
40	4	7	9
44	5	9	10
48	5	8	11
52	4	7	8
56	7	14	16
60	4	6	11
64	14	10	11
68	6	14	12
72	14	19	23
76	16	37	38
80	7	11	15
84	8	13	15
88	6	10	20
92	7	10	14

DATE: 5-26-71
SPT Boring Log
Hole BB-1

Depth, ft.	Blows		
	6" seating	1st 6"	2nd 6"
4	3	7	8
8	5	6	7
12	5	7	8
16	5	7	7
20	7	10	11
24	8	13	17
28	8	15	13
32	11	13	14
36	14	28	72 (3½)
40	17 (3½)	50 (5½)	50 (1 3/4)
44	12 (3½)	50 (6)	50 (4)
48	12 (4½)	28	32
52	13 (4)	26	25
56	31	35	50 (5 3/4)
60	26	23	27
64	31	50 (4½)	50 (2½)

LABORATORY LOG OF BORING #G-1-2									
FOR									
I-610 & I-45 INTERCHANGE									
DATE	May 21, 1971		TYPE	THD Penetrometer		LOCATION	N 695,995 E 3,177,460		
DEPTH FEET	SYMBOL	CORES	DESCRIPTION	BLOWS PER FOOT		COHESION P.S.I.	FRICTION ANGLE	UNIT DRY WT LBS/CU.FT.	POINT BEARING T.S.F.
				1st 6"	2nd 6"				1.0 2.0 3.0 4.0 5.0
ELEVATION+ 41.6								MOISTURE CONTENT	
								10 20 30 40 50	
0			Dk. gray tan silty clay	4	2				
10			Tan lt. gray w/calc. @ 8'	3	4				
			Lt. gray tan w/o calc. @ 12'	7	8				
				7	9				
20			Tan lt. gray clayey silt w/calc. w/o calc. @ 20'	8	7				
				12	17				
30			Tan lt. gray silty clay Red lt. gray @ 26'	9	12				
				9	12				
				9	12				
40			Tan lt. gray silty sand 8" layer clay @ 40'	27	26				
				19	21				
				31	36				
50			Lt. gray tan @ 49'	35	32				
			Tan lt. gray @ 52'	26	34				
60				4½"	3½"				
				6"	2½"				
				4½"	3½"				
70				5"	3½"				
				2½"	1"				
				2½"	1½"				

W
A
T
E
R



LABORATORY LOG OF BORING G-2-2									
FOR									
I-610 & I-45 Interchange									
DATE May 18, 1971		TYPE 3" Shelby		LOCATION N 696,375 E 3,178,500					
DEPTH FEET	SYMBOL	CORES	DESCRIPTION	BLOWS PER FOOT		COHESION P.S.I.	FRICTION ANGLE	UNIT DRY WT. LBS./CU. FT.	POINT BEARING T.S.F.
				1st 6"	2nd 6"				1.0 2.0 3.0 4.0 5.0
			ELEVATION+ 39.6					MOISTURE CONTENT	
								10 20 30 40 50	
0			Dk. gray tan silty clay Tan lt. gray @ 4' W/silt pockets @ 6'					96	
10			Tan lt. gray clayey silt w/ layers of clay					106	
20			Tan lt. gray silty clay Lt. gray tan @ 14' Tan lt. gray @ 15' Red lt. gray @ 17'					104	
30			Red lt. gray clayey silt w/ clay layers					99	
40			Tan lt. gray silty clay w/ calc. @ 24' Red lt. gray @ 27' W/ calc. @ 29'					96	
50			3" layer silt @ 31' 2" layer silt @ 32'					108	
60			Tan lt. gray @ 50' Dk. gray tan @ 52'					98	
70			Gray tan silty sand 8" layer very sandy clay @ 62' 7" layer very sandy clay @ 63'					95	
80			Dk. gray tan silty clay					94	
90			Gray tan silty sand					78	
100			4" layer clay @ 76'					102	
110			Red lt. gray silty clay					100	
120			1" layer silt @ 85' 2" layer silt @ 86' 1" layer silt @ 88'					101	
130			Red lt. gray clayey silt					95	
			• Slickensided						

W
A
T
E
R

LABORATORY LOG OF BORING #G-2-3									
FOR									
I-610 & I-45 INTERCHANGE									
N 696,375									
LOCATION E 3,178,525									
DATE May 19, 1971									
TYPE Penetrometer									
DEPTH FEET	SYMBOL CORES	DESCRIPTION	BLOWS PER FOOT		COHESION P.S.I.	FRICTION ANGLE	UNIT DRY WT. LBS./CU. FT.	POINT BEARING T.S.F.	
			1st 6"	2nd 6"				1.0	2.0
		ELEVATION+ 39.4							MOISTURE CONTENT
								10 20 30 40 50	
0		Dk. gray tan silty clay							
		Tan lt. gray @ 4'	7	5					
		W/silt layers @ 7'							
10		W/calc. @ 10'	3	4					
		W/o silt layers @ 13'	5	6					
20		Red lt. gray @ 18'	8	10					
			11	10					
			10	11					
30			10	12					
		8" layer silt @ 32'	20	18					
			12	13					
40			12	12					
			13	13					
50		Lt. gray @ 50'	14	14					
		Dk. gray @ 54'	10	12					
60		Dk. gray tan silty sand	16	15					
			30	34					
			20	15					
70			14	14					
			20	19					
			3 1/2"	6"					
80		Red lt. gray silty clay	13	18					
			13	12					
			19	81					
90		Red lt. gray clayey silt							
		Red lt. gray silty clay	19	18					

W
A
T
E
R

LABORATORY LOG OF BORING #B-B-2									
FOR									
STATE HIGHWAY 288									
DATE		May 27, 1971		TYPE		3" Shelby		LOCATION	
								N 700,965 E 3,149,205	
DEPTH FEET	SYMBOL	CORES	DESCRIPTION	BLOWS PER FOOT		COHESION P.S.I.	FRICTION ANGLE	UNIT DRY WT LBS./CU.FT.	POINT BEARING T.S.F.
				1st 6"	2nd 6"				1.0 2.0 3.0 4.0 5.0
			ELEVATION+ 50.0					MOISTURE CONTENT	
								10 20 30 40 50	
0			Gray tan silty clay w/calc.						
			Lt. gray tan @ 5'					110	
10			Tan lt. gray clayey silt w/calc.					118	
			Tan lt. gray very silty clay w/calc. & sand pockets					118	
20			Lt. gray tan @ 18'						
			W/o sand pockets @ 18 1/2'						
			Lt. gray tan sandy clay w/calc.					119	
			Very sandy @ 27'						
30			Tan lt. gray clayey sand					118	
								114	
			Tan lt. gray silty sand					111	
				32	49				
40				2"	1/2"				
				2"	3"				
50				3 1/2"	1 3/4"				
			8" layer sand stone @ 53'	4 1/2"	1/2"				
				1"	3/4"				
60				5 1/2"	2 1/4"				
				5 1/2"	1 1/4"				
70			• Slickensided						

W
A
T
E
R

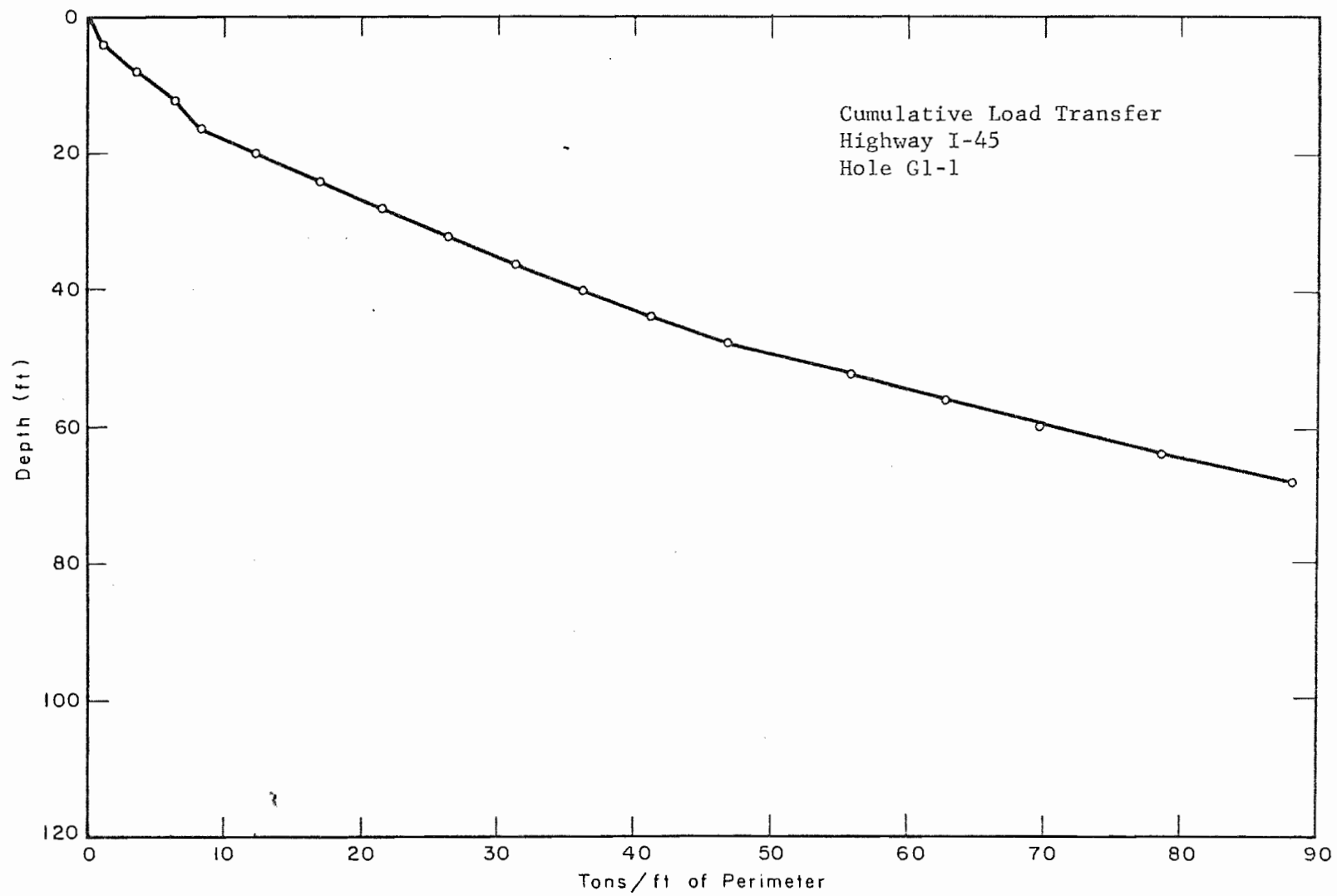
LABORATORY LOG OF BORING B-B-3									
FOR									
STATE HIGHWAY 288									
N 700,960									
E 3,149,215									
DATE May 28, 1971 TYPE THD Penetrometer LOCATION									
DEPTH FEET	SYMBOL	CORES	DESCRIPTION	BLOWS PER FOOT		COHESION P.S.I.	FRICTION ANGLE	UNIT DRY WT. LBS/CU. FT.	POINT BEARING T.S.F.
				1st 6"	2nd 6"				1.0 2.0 3.0 4.0 5.0
ELEVATION+ 50.1								MOISTURE CONTENT	
								10 20 30 40 50	
0			Gray tan silty clay w/calc. Lt. gray tan @ 4'	13	14				
10			Tan lt. gray clayey silt	11	9				
20			Lt. gray tan silty clay w/vertical silt seams	9	12				
				16	21				
				9	19				
30			Lt. gray tan clayey sand	41	49				
			Lt. gray tan silty sand	24	29				
40				48	52				
				2"	1"				
				2½"	1½"				
50				3½"	2"				
				1½"	1½"				
60				3½"	3½"				
70									

W
A
T
E
R

APPENDIX II
TEST SHAFTS DESIGN SHEETS

CALCULATION OF SIDE FRICTION BY SPT, HOLE G1-1

Depth (feet)	O.B. psi	N(SPT) (Blows/ft)	ϕ deg.	S tsf	Sep. T/ft, perimeter	Accum. T/ft, perimeter
4	3.3	5		.33	1.32	1.32
8	6.7	9		.60	2.40	3.72
12	9.7	11		.73	2.92	6.64
16	12.8	7		.47	1.68	8.32
20	14.5	16		1.07	4.28	12.60
24	16.3	17		1.13	4.52	17.12
28	18.0	18		1.19	4.76	21.88
32	19.5	17		1.13	4.53	26.41
36	21.4	31	40	1.25	5.00	31.41
40	23.4	25	38	1.31	5.24	36.65
44	25.6	12	34	1.24	4.96	41.61
48	27.4	14	34	1.33	5.32	46.93
52	29.1	23	36	1.51	6.04	55.97
56	31.2	31	38	1.75	7.00	62.97
60	33.0	24	36	1.72	6.88	69.85
64	34.9	53	42	2.25	9.00	78.85
68	36.7	77	42	2.38	9.52	88.37
72	38.7	61				
76	40.6	43				

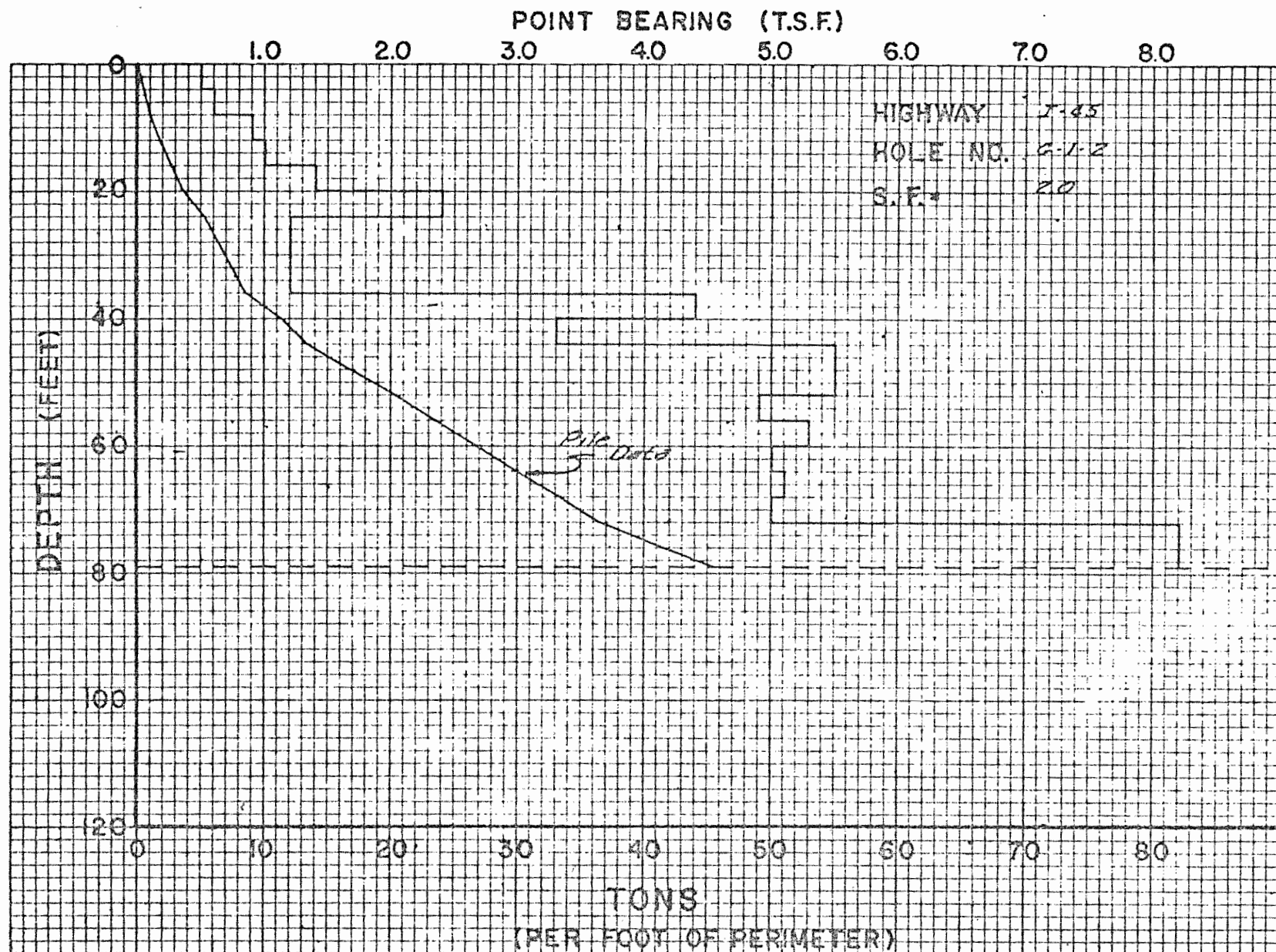


TEXAS HIGHWAY DEPARTMENT
HOUSTON URBAN EXPRESSWAYS

Project I-45
Hole G1-2

FOUNDATION DESIGN CALCULATIONS

Depth		Unit Wt.		O.B. Press.		Pen. Value	ϕ	Tan ϕ	C	Shear Resist.		Skin Frict.		Point Resist.
From	To	Total	Subm.	Sep.	Accum.	Blows	deg.		psi	psi	tsf	Pf = S X H	Sep.	tsf
ft.	ft.	pcf	pcf	psi	psi	ft.				SF.=2.0		T/f*	T/f*	
											11(.072)	12(2-1)		
0	4					6		clay			.117	0.47	0.47	0.5
4	8					7		clay			.140	0.56	1.03	0.6
8	12					15		clay			.210	0.84	1.87	0.9
12	16					16		clay			.233	0.93	2.80	1.0
16	20					15		clay			.221	0.88	3.68	1.4
20	24					29					.379	1.52	5.20	2.4
24	28					21		clay			.280	1.12	6.32	1.2
28	32					21		clay			.280	1.12	7.44	1.2
32	36					21		clay			.280	1.12	8.56	1.2
36	40					53					.695	2.78	11.34	4.4
40	44					40					.521	2.08	13.42	3.3
44	48					67					.869	3.48	16.90	5.5
48	52					67					.869	3.48	20.38	5.5
52	56					60					.774	3.10	23.48	4.9
56	60					7.75"					.837	3.35	26.83	5.3
60	64					8.75"					.790	3.16	29.99	5.0
64	68					8.75"					.806	3.22	33.21	5.1
68	72					8.75"					.790	3.16	36.37	5.0
72	76					3.25"					1.296	5.18	41.55	8.2(12.9)
76	79					3.5"					1.296	3.89	45.44	8.2(11.9)



TEXAS HIGHWAY DEPARTMENT
HOUSTON URBAN EXPRESSWAYS

Project I-45
Hole G1-3

FOUNDATION DESIGN CALCULATIONS

Depth		Unit Wt.		O.B. Press.		Pen. Value	ϕ	Tan ϕ	C	Shear Resist.		Skin Frict.		Point Resist.
From	To	Total	Subm.	Sep.	Accum.	Blows	deg.		psi	S=C+Ntan ϕ		Pf = S X H		
ft.	ft.	pcf	pcf	psi	psi	ft.				SF.= 2.0	tsf	Sep. T/f*	Accum. T/f*	tsf
										11(.072)		12(2-1)		
0	2	120.69		1.68	1.68		15	.268	14	7.23	.520	1.04	1.04	2.9
2	6	115.59		3.21	4.89		1	.017	2	1.04	.075	0.30	1.34	0.3
6	9	119.40		2.49	7.38		0	.000	3	1.50	.108	0.32	1.66	0.4
9	10	118.18		0.82	8.20		4	.070	5	2.79	.200	0.20	1.86	0.8
10	11	120.32		0.84	9.04		4	.070	5	2.82	.203	0.20	2.06	0.8
11	13	118.76		1.65	10.69		6	.105	3	2.06	.148	0.30	2.36	0.6
13	14	120.47		0.84	11.53		3	.052	5	2.80	.202	0.20	2.36	0.7
14	15	125.79		0.87	12.40		8	.141	6	3.87	.279	0.28	2.84	1.2
15	16	125.45		0.44	12.48		7	.123	1	1.29	.093	0.09	2.93	0.4
16	17	115.94		0.37	13.21	** 15.					.205	0.21	3.14	1.3
17	19	127.80		0.91	14.12		6	.105	2	1.74	.125	0.25	3.39	0.5
19	20	122.31		0.42	14.54	** 15.					.205	0.21	3.60	1.3
20	22	127.37		0.90	15.44		1	.017	1	0.63	.045	0.09	3.69	0.2
22	23	126.48		0.44	15.88		12	.212	8	5.68	.409	0.41	4.10	2.0
23	24	123.81		0.43	16.31		1	.017	15	7.64	.550	0.55	4.65	1.9
24	26	122.48		0.83	17.14		11	.194	8	5.66	.403	0.82	5.47	1.9
26	27	121.62		0.41	17.55		12	.212	6	4.86	.350	0.35	5.82	1.7
27	28	121.44		0.41	17.96		9	.158	9	5.92	.426	0.43	6.25	1.9
28	30	116.31		0.75	18.71		5	.087	5	3.31	.239	0.48	6.73	0.9

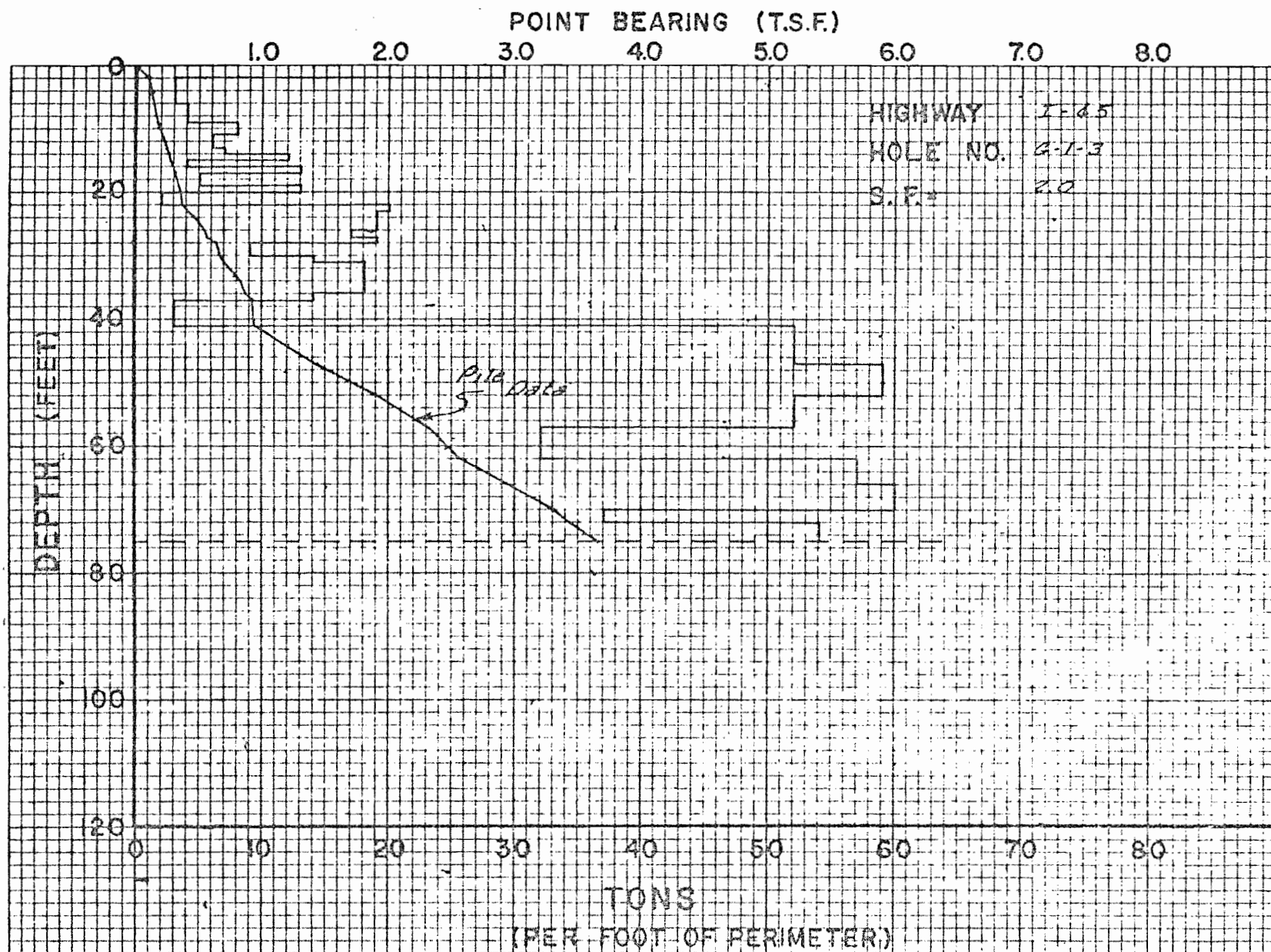
TEXAS HIGHWAY DEPARTMENT
HOUSTON URBAN EXPRESSWAYS
FOUNDATION DESIGN CALCULATIONS

Project I-45
Hole G1-3

Depth		Unit Wt.		O.B. Press.		Pen.	ϕ	Tan	C	Shear Resist.	Skin Frict.	Point Resist.		
From	To	Total	Subm.	Sep.	Accum.	Value		ϕ		$S=C+N\tan\phi$	Pf.= S X H			
ft.	ft.	pcf	pcf	psi	psi	Blows	deg.		psi	psi	tsf	Sep.	Accum.	
						ft.						T/f*	T/f*	
										11(.072)	12(2-1)			
30	31	121.15		0.41	19.12		8	.141	6	4.35	.313	0.31	7.04	1.4
31	33	122.67		0.84	19.96		5	.087	11	6.37	.459	0.92	7.96	1.8
33	34	132.35		0.49	20.45	** 21					.284	0.28	8.24	1.8
34	36	129.25		0.93	21.38	** 21					.284	0.57	8.81	1.8
36	37	132.25		0.48	21.86		15	.268	1	3.43	.247	0.25	9.06	1.4
37	41	134.67		2.00	23.86		3	.052	1	1.12	.081	0.32	9.38	0.3
41	47	131.61		2.88	26.74	63					.822	4.93	14.31	5.2
47	52	131.61		2.40	29.14	72					.932	4.66	18.97	5.9
52	57	131.61		2.40	31.54	63					.822	4.11	23.08	5.2
57	62	131.61		2.40	33.94	39					.506	2.53	25.61	3.2
62	66	131.61		1.92	35.86	70					.901	3.60	29.21	5.7
66	70	131.61		1.92	37.78	6.5"					.948	3.79	33.00	6.0
70	72	131.61		0.96	38.74	45					.585	1.17	34.17	3.7
72	75	131.61		1.44	40.18	7.5"					.853	2.56	36.73	5.4

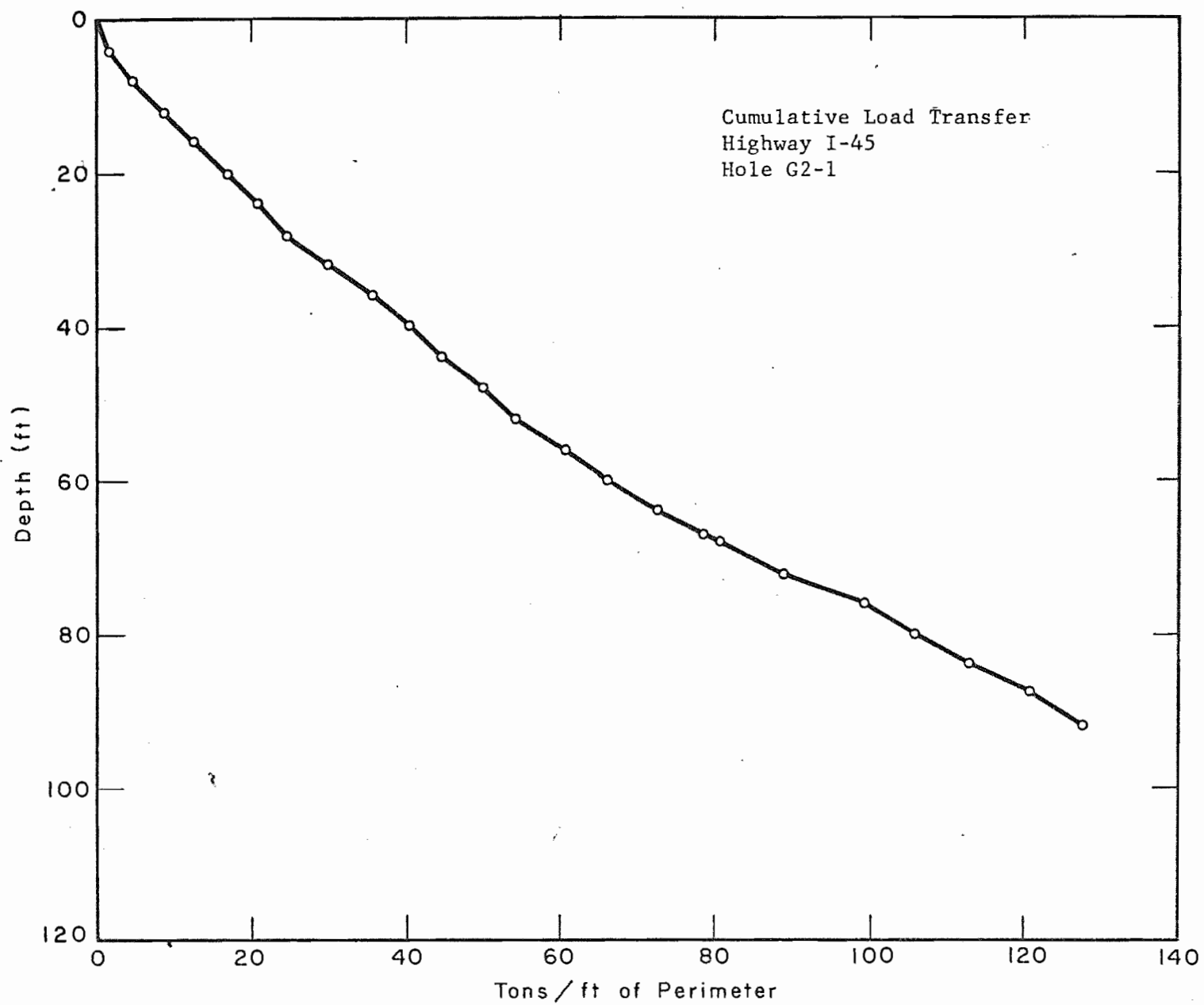
*Tons per ft. of perimeter

**Penetrometer values taken from approx. depth from hole G1-2.



CALCULATION OF SIDE FRICTION BY SPT, HOLE G2-1

Depth (feet)	O.B. psi	N(SPT) (Blows/ft)	ϕ deg.	S tsf	Sep. T/ft, perimeter	Accum. T/ft, perimeter
4	Assuming an average density of 122.0 pcf and a water table at 13 feet.	5		.33	1.32	1.32
8		14		.93	3.72	5.04
12		14		.93	3.72	8.76
16		15		1.00	4.00	12.76
20		18		1.20	4.80	17.50
24		12		.80	3.20	20.70
28		14		.93	3.72	24.42
32		22		1.47	5.88	30.30
36		21		1.40	5.60	35.90
40		16		1.07	4.28	40.18
44		19		1.27	5.08	45.26
48		19		1.27	5.08	50.34
52		15		1.00	4.00	54.34
56		30		2.00	8.00	60.34
60	31.0	17	35	1.57	6.28	66.62
64	32.6	21	35	1.65	6.60	73.22
68	34.2	26	37	1.85	7.40	80.62
72	35.8	42	41	2.24	8.96	89.58
76	37.4	75	42	2.41	9.64	99.22
80		26		1.73	6.92	106.14
84		28		1.87	7.48	113.62
88		30		2.00	8.00	121.62



Project I-45
Hole G2-2

65

TEXAS HIGHWAY DEPARTMENT
HOUSTON URBAN EXPRESSWAYS
FOUNDATION DESIGN CALCULATIONS

Project I-45
Hole G2-2

Depth		Unit Wt.		O.B. Press.		Pen. Value	ϕ	Tan ϕ	C	Shear Resist.		Skin Frict.		Point Resist.
From	To	Total	Subm.	Sep.	Accum.	Blows				$S=C+N\tan\phi$		Pf = S x H		
ft.	ft.	pcf	pcf	psi	psi	ft.	deg.		psi	psi	tsf	T/f*	T/f*	tsf
						**						11(.072)	12(2-1)	
27	28	128.42		0.46	15.23		17	.306	8	6.33	.456	0.46	6.90	2.8
28	29	131.58		0.48	15.71		3	.052	12	6.41	.461	0.46	7.36	1.7
29	30	131.69		0.48	16.19		17	.306	9	6.98	.502	0.50	7.86	3.0
30	31	127.38		0.45	16.64		10	.176	11	6.96	.501	0.50	8.36	2.3
31	33	128.17		0.91	17.55		8	.148	3	2.80	.202	0.40	8.76	0.9
33	34	127.20		0.45	18.00		15	.268	8	6.41	.462	0.46	9.22	2.6
34	35	123.98		0.43	18.43		10	.178	13	8.14	.586	0.59	9.81	2.7
35	36	126.46		0.44	18.87		12	.212	8	6.00	.432	0.43	10.24	2.1
36	37	121.36		0.41	19.28		9	.158	10	6.52	.470	0.47	10.71	2.1
37	39	125.11		0.87	20.15		12	.212	9	6.64	.473	0.96	11.67	2.3
39	40	122.41		0.42	20.57		5	.087	12	6.89	.496	0.50	12.17	1.9
40	41	120.50		0.40	20.97		2	.035	9	4.87	.350	0.35	12.52	1.3
41	42	132.35		0.49	21.46		7	.123	8	5.32	.383	0.33	12.90	1.6
42	43	123.60		0.42	21.88		8	.141	16	9.54	.687	0.69	13.59	3.0
43	44	132.35		0.49	22.37		7	.123	9	5.88	.423	0.42	14.01	1.8
44	46	123.98		0.85	23.22		9	.158	10	6.83	.492	0.98	14.99	2.2
46	47	118.90		0.39	23.61		6	.105	8	5.24	.377	0.38	15.37	1.5
47	48	121.51		0.41	24.02		16	.287	8	7.45	.536	0.54	15.91	3.1
48	49	120.45		0.40	24.42		8	.141	10	6.72	.484	0.48	16.39	2.1
49	51	117.87		0.77	25.19		7	.123	10	6.55	.472	0.94	17.33	2.0
51	52	118.37		0.39	25.58		7	.123	8	5.57	.401	0.40	17.73	1.7

TEXAS HIGHWAY DEPARTMENT
HOUSTON URBAN EXPRESSWAYS
FOUNDATION DESIGN CALCULATIONS

Project I-45
Hole G2-2

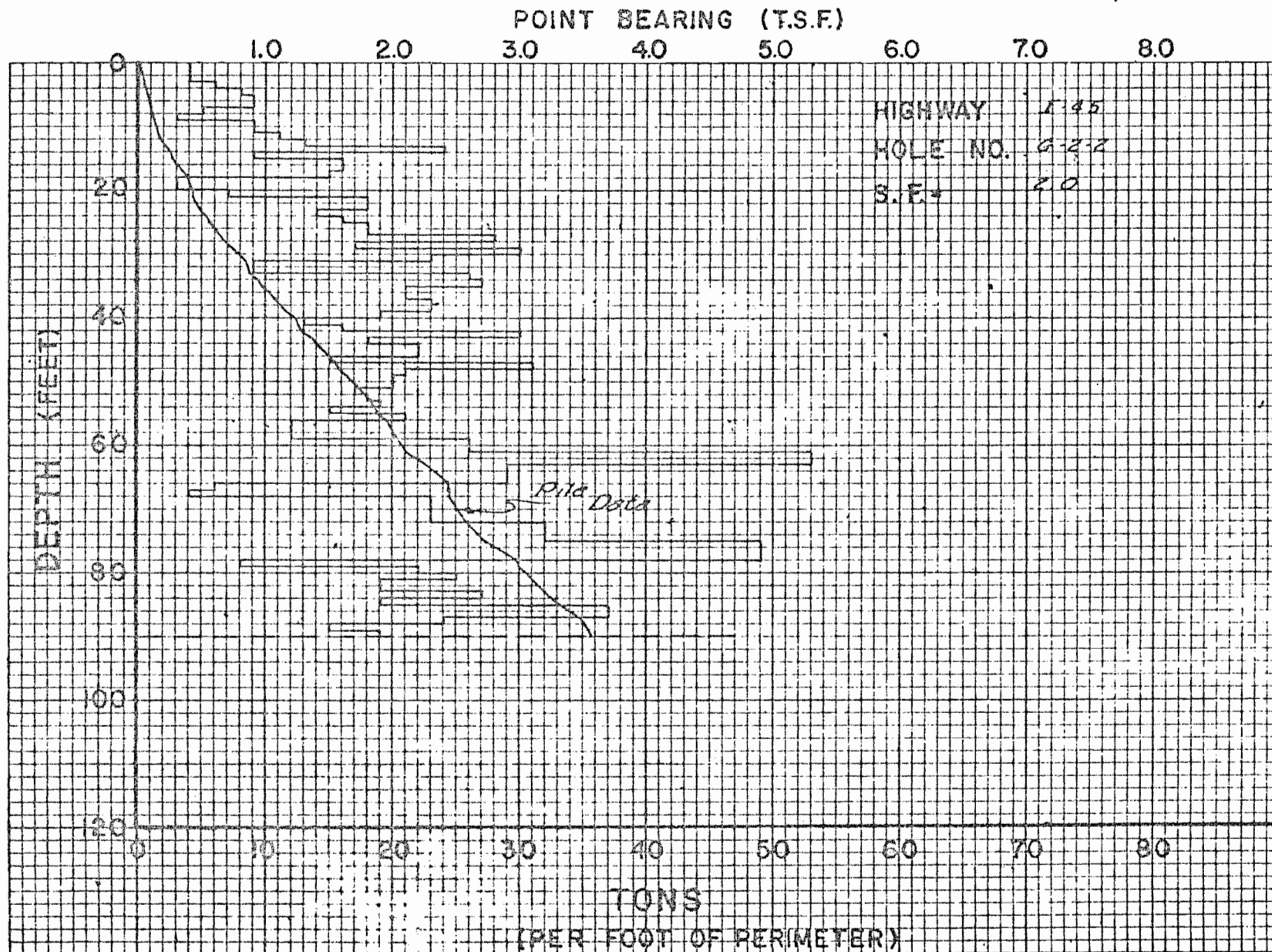
Depth		Unit Wt.		O.B. Press.		Pen.	ϕ	Tan	C	Shear Resist.	Skin Frict.	Point	
From	To	Total	Subm.	Sep.	Accum.	Value		ϕ		$S=C+N\tan\phi$	$P_f = S \times H$	Sep.	Accum.
ft.	ft.	pcf	pcf	psi	psi	Blows	deg.		psi	psi	tsf	T/f*	T/f*
						ft.							tsf
						**							
11(.072)12(2-1)													
52	53	120.30		0.40	25.98		8	.141	8	5.83	.420	0.42	18.15
53	54	118.60		0.39	26.37		10	.176	7	5.82	.419	0.42	18.57
54	55	112.49		0.35	26.72		7	.123	7	5.14	.370	0.37	18.94
55	56	111.00		0.34	27.06		10	.176	8	6.38	.459	0.46	19.40
56	59	105.41		0.89	27.95		5	.087	6	4.22	.304	0.91	20.31
59	61	114.61		0.72	28.67	31					.411	0.82	21.13
61	63	127.04		0.90	29.57	64					.837	1.67	22.80
63	66	123.94		1.28	30.85	35					.458	1.37	24.17
66	67	105.50		0.30	31.15		4	.070	2	2.09	.150	0.15	24.32
67	68	108.83		0.32	31.47		0	.000	3	1.50	.108	0.11	24.43
68	71	115.72		1.11	32.58	28					.363	1.09	25.52
71	72	132.74		0.49	33.07	28					.363	0.36	25.88
72	74	126.03		0.88	33.95	39					.506	1.01	26.89
74	75	108.05		0.32	34.27	39					.506	0.51	27.40
75	77	133.84		0.99	35.26	9.75"					.774	1.55	28.95
77	78	126.94		0.45	35.71	9.75"					.774	0.77	29.72
78	79	126.36		0.44	36.15		2	.035	5	3.13	.226	0.23	29.95
79	80	114.44		0.36	36.51		7	.123	10	7.25	.522	0.52	30.47
80	81	141.80		0.55	37.06		8	.141	11	8.11	.584	0.58	31.05
81	83	122.22		0.83	37.89		4	.070	11	6.83	.491	0.98	32.03
83	84	123.75		0.43	38.32		9	.158	11	8.53	.614	0.61	32.64

TEXAS HIGHWAY DEPARTMENT
HOUSTON URBAN EXPRESSWAYS
FOUNDATION DESIGN CALCULATIONS

Project I-45
Hole G2-2

Depth		Unit Wt.		O.B. Press.		Pen. Value	ϕ	Tan ϕ	C	Shear Resist.		Skin Frict.		Point Resist.
From	To	Total	Subm.	Sep.	Accum.	Blows				$S=C+N\tan\phi$		Pf = S x H		
ft.	ft.	pcf	pcf	psi	psi	ft.	deg.		psi	psi	tsf	T/f*	T/f*	tsf
						**								
											11(.072)	12(201)		
84	85	128.61		0.46	38.78		6	.105	9	6.54	.471	0.47	33.11	1.9
85	87	129.86		0.94	39.72		13	.231	11	10.09	.726	1.45	34.56	3.7
87	88	129.01		0.46	40.18		10	.176	7	7.04	.507	0.51	35.07	2.4
88	89	126.29		0.44	40.62		7	.123	5	5.00	.360	0.36	35.42	1.5
89	90	116.79		0.38	41.00		13	.231	1	5.24	.377	0.38	35.80	1.9

**All pen test taken from approx. depth from hole G2-3



TEXAS HIGHWAY DEPARTMENT
HOUSTON URBAN EXPRESSWAYS
FOUNDATION DESIGN CALCULATIONS

Project I-45
Hole G2-3

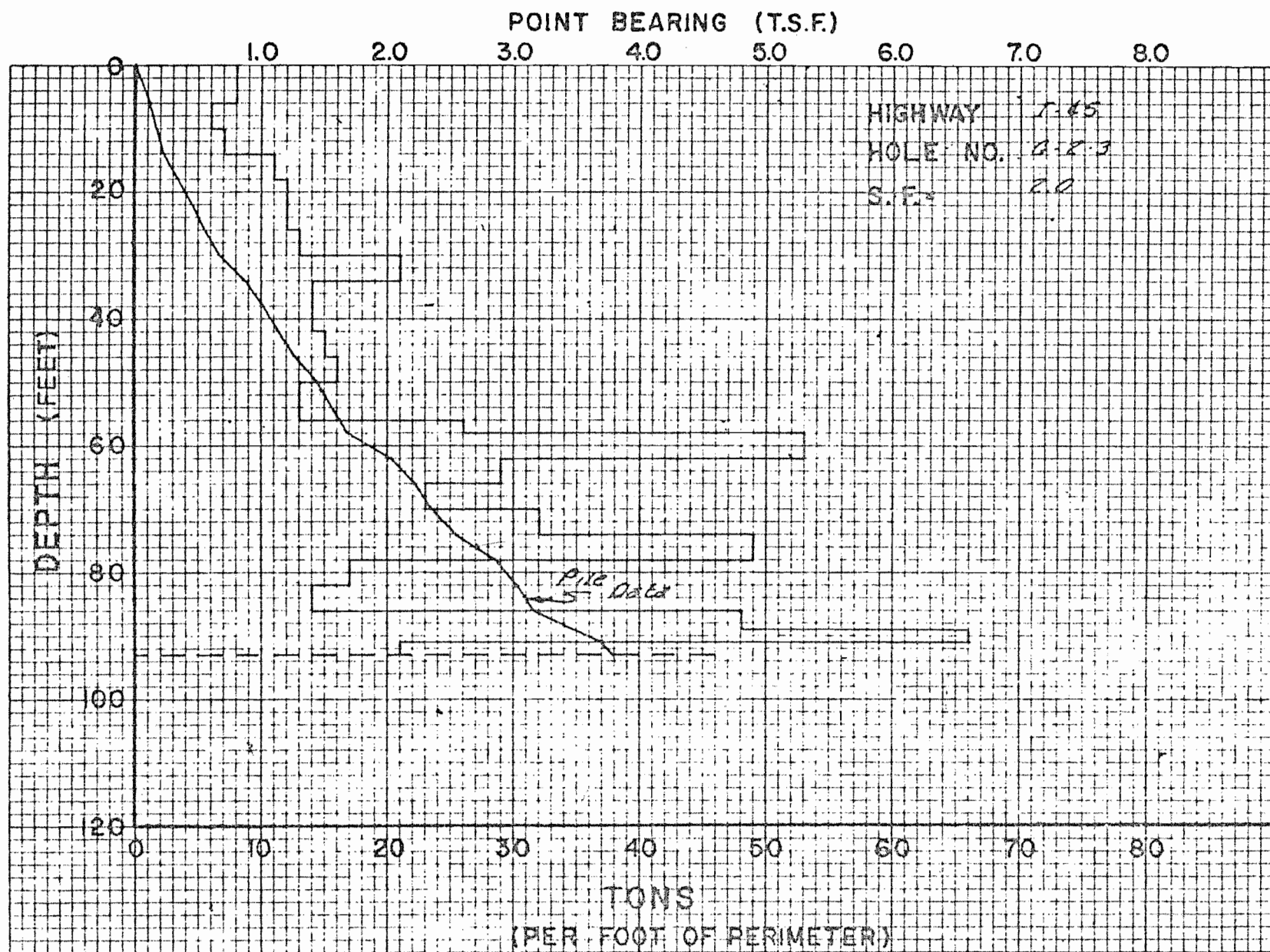
Depth		Unit Wt.		O.B. Press.		Pen. Value	ϕ	Tan ϕ	C	Shear Resist.	Skin Frict.		Point Resist.
From	To	Total	Subm.	Sep.	Accum.	Blows	deg.		psi	$S=C+N\tan\phi$	Pf = S x H		
ft.	ft.	pcf	pcf	psi	psi	ft.				SF. = 2.0	Sep.	Accum.	
										tsf	T/f*	T/f*	tsf
										11(.072)	12(2-1)		
0	6					12				0.186	1.12	1.12	0.8
6	10					7				.140	0.56	1.68	0.6
10	14					11				.163	0.65	2.33	0.7
14	18					18				.256	1.02	3.35	1.1
18	22					21				.280	1.12	4.47	1.2
22	26					21				.280	1.12	5.59	1.2
26	30					22				.303	1.21	6.80	1.3
30	34					38				.489	1.96	8.76	2.1
34	38					25				.326	1.30	10.06	1.4
38	42					24				.326	1.30	11.36	1.4
42	46					26				.350	1.40	12.76	1.5
46	50					28				.373	1.49	14.25	1.6
50	56					22		clay		.303	1.82	16.07	1.3
56	58					31				.411	0.82	16.89	2.6
58	62					64				.837	3.35	20.24	5.3
62	66					35				.458	1.83	22.07	2.9
66	70					28				.363	1.45	23.52	2.3
70	74					39				.506	2.02	25.54	3.2
74	78					9.75"				.774	3.10	28.64	4.9
78	82					31				.396	1.58	30.22	17.
82	86					25				.326	1.30	31.52	1.4

TEXAS HIGHWAY DEPARTMENT
HOUSTON URBAN EXPRESSWAYS
FOUNDATION DESIGN CALCULATIONS

Project I-45
Hole G2-3

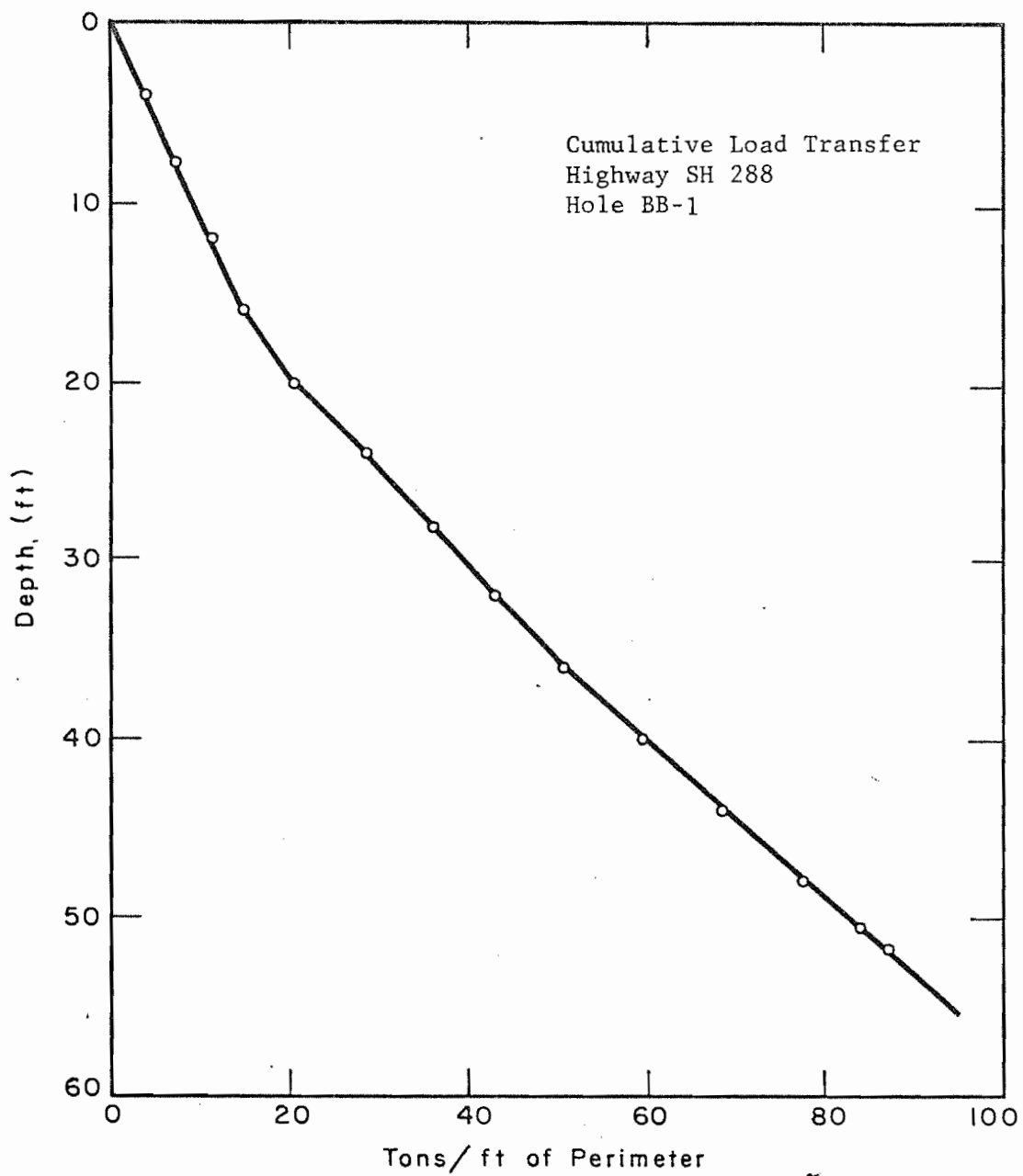
Depth		Unit Wt.		O.B. Press.		Pen.	ϕ	Tan	C	Shear Resist.	Skin Frict.		Point
						Value		ϕ		$S=C+N\tan\phi$	$P_f = S \times H$		Resist.
From	To	Total	Subm.	Sep.	Accum.	Blows				SF.= 2.0	Sep.	Accum.	
ft.	ft.	pcf	pcf	psi	psi	ft.	deg.		psi	psi	tsf	T/f*	T/f*
										11(.072)	12(2-1)		
86	89					11.5"		clay		1.118	3.35	34.87	4.8
89	91					** 80				1.043	2.09	36.96	6.6
91	93					37		clay		.489	0.98	37.94	2.1

**Estimated



CALCULATION OF SIDE FRICTION BY SPT, HOLE BB-1

Depth (feet)	O.B. psi	N(SPT) (Blows/ft)	ϕ deg.	S tsf	Sep. T/ft, perimeter	Accum. T/ft, perimeter
4	3.79	15		1.00	4.00	4.00
8	7.57	13		.87	3.48	7.48
12	11.22	15		1.00	4.00	11.48
16	14.98	14		.93	3.72	15.20
20	18.80	21		1.40	5.60	20.80
24	22.6	30		2.00	8.00	28.80
28	26.36	28		1.87	7.48	36.28
32	28.6	27	41	1.79	7.16	43.44
36	30.6	100(9½")	42	1.97	7.88	51.32
40	32.3	100(7½")	42	2.08	8.32	59.64
44	34.2	100(10")	42	2.20	8.80	68.44
48	36.0	60	42	2.32	9.28	77.72
52	38.01	51	42	2.46	9.84	87.56
56	39.87	88	42	2.58	10.32	97.88



TEXAS HIGHWAY DEPARTMENT
HOUSTON URBAN EXPRESSWAYS
FOUNDATION DESIGN CALCULATIONS

Project I-45
Hole BB-2

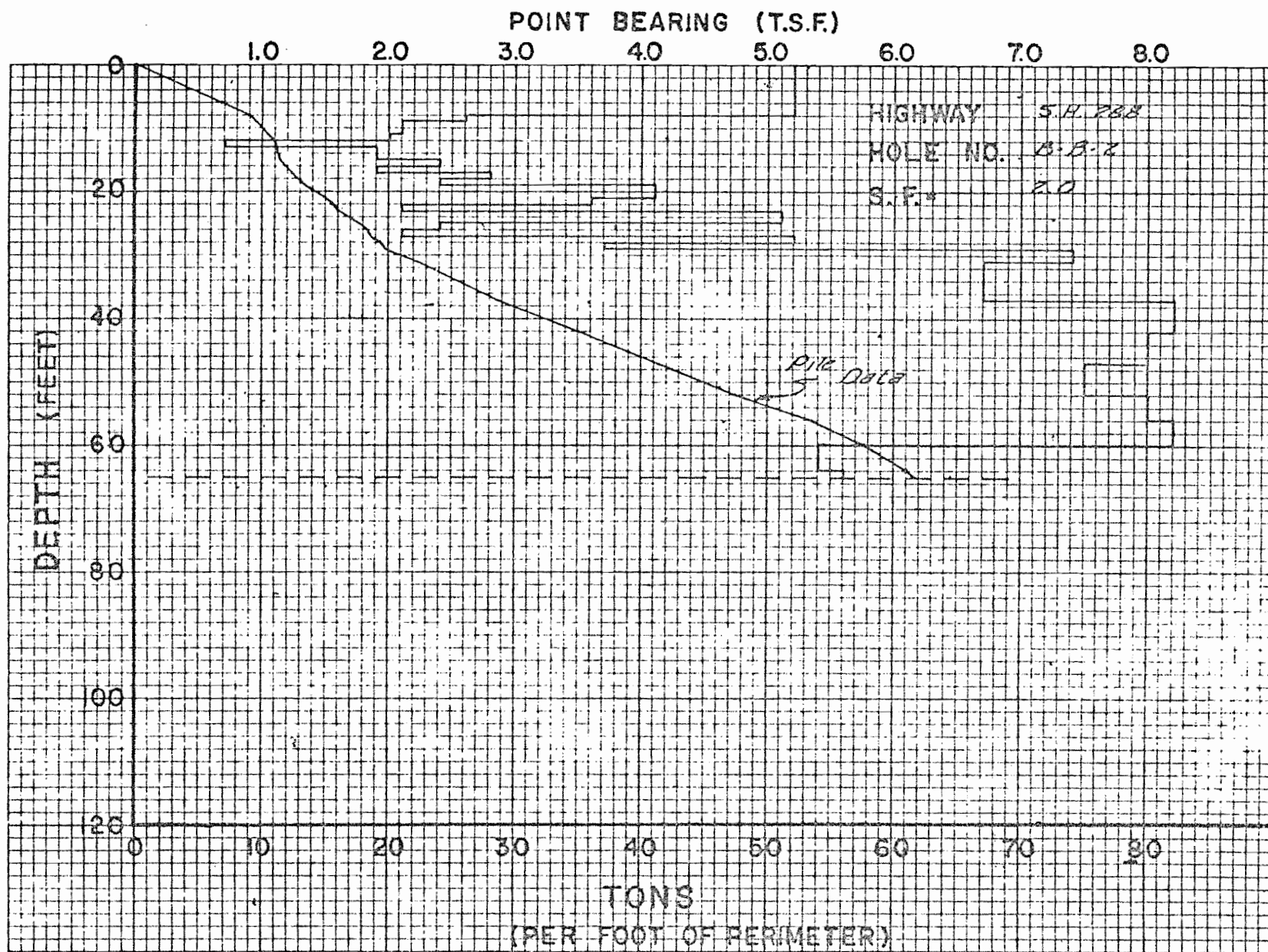
Depth		Unit Wt.		O.B. Press.		Pen. Value	ϕ	Tan ϕ	C	Shear Resist.		Skin Frict.		Point Resist.
From	To	Total	Subm.	Sep.	Accum.	Blows	deg.		psi	S=C+Ntan ϕ	SF.= 2.0	Pf = S X H	Sep. Accum.	
ft.	ft.	pcf	pcf	psi	psi	ft.				psi	tsf	T/f*	T/f*	tsf
											11(.072)	12(2-1)		
0	8	136.24		7.57	7.57		10	.176	30	15.67	1.128	9.02	9.02	5.2
8	9	133.61		0.93	8.50		12	.212	13	7.40	.533	0.53	9.55	2.6
9	11	132.83		1.84	10.34		11	.194	10	6.00	.432	0.86	10.41	2.1
11	12	127.00		0.88	11.22		8	.141	11	6.29	.453	0.45	10.86	2.0
12	13	135.02		0.94	12.16		16	.287	0	1.74	.126	0.13	10.99	0.7
13	15	135.21		1.88	14.04		24	.445	0	3.12	.225	0.45	11.44	1.7
15	16	136.01		0.94	14.98		14	.249	9	6.37	.458	0.46	11.90	2.4
16	17	132.57		0.92	15.90		17	.306	4	4.43	.319	0.32	12.22	1.9
17	18	133.26		0.93	16.83		18	.325	7	6.23	.449	0.45	12.67	2.8
18	19	140.27		0.97	17.80		1	.017	19	9.65	.695	0.69	13.37	2.4
19	21	136.98		1.90	19.70		12	.212	19	11.59	.834	1.67	15.04	4.1
21	22	137.44		0.95	20.65		22	.404	5	6.67	.480	0.48	15.52	3.6
22	23	139.89		0.97	21.62	** 37					.489	0.49	16.01	2.1(clay)
23	25	137.83		1.91	23.53		17	.306	16	11.60	.835	1.67	17.68	5.1
25	26	138.86		0.96	24.49		10	.176	10	7.16	.515	0.52	18.20	2.4
26	27	135.96		0.94	25.43		10	.176	8	6.24	.449	0.45	18.65	2.1
27	28	135.91		0.94	26.36		22	.404	9	9.82	.707	0.71	19.36	5.2
28	29	135.58		0.94	27.31		20	.364	5	7.47	.538	0.54	19.90	3.7
29	31	130.85		0.95	28.26	** 90					1.169	2.34	22.24	7.4

TEXAS HIGHWAY DEPARTMENT
HOUSTON URBAN EXPRESSWAYS
FOUNDATION DESIGN CALCULATIONS

Project I-45
Hole BB-2

Depth		Unit Wt.		O.B. Press.		Pen. Value	ϕ	Tan ϕ	C	Shear Resist.	Skin Frict.		Point Resist.
From	To	Total	Subm.	Sep.	Accum.	Blows	deg.		psi	$S=C+N\tan\phi$ SF.= 2.0	Pf = S x H	Sep. Accum.	
ft.	ft.	pcf	pcf	psi	psi	ft.				psi	tsf	T/f* T/f*	tsf
											11(.072)	12(2-1)	
31	37	129.41		2.79	31.05	81					1.059	6.35 28.59	6.7
37	42	129.41		2.32	33.37	2.5"					1.296	6.48 35.07	8.2(16.4)
42	47	129.41		2.32	35.69	5.0"					1.264	6.32 41.39	8.0
47	52	129.41		2.32	38.01	5.25"					1.185	5.93 47.32	7.5
52	56	129.41		1.86	39.87	5.0"					1.264	5.06 52.38	8.0
56	60	129.41		1.86	41.73	1.75"					1.296	5.18 57.56	8.2(22.5)
60	64	129.41		1.86	43.59	7.5"					.853	3.41 60.97	5.4
64	65	129.41		0.46	44.05	7.0"					.885	0.88 61.85	5.6

**Penetrometer test taken from approx. depth from hole BB-3.



TEXAS HIGHWAY DEPARTMENT
HOUSTON URBAN EXPRESSWAYS
FOUNDATION DESIGN CALCULATIONS

Project I-45
Hole BB-3

Depth		Unit Wt.		O.B. Press.		Pen. Value	ϕ	Tan ϕ	C	Shear Resist.	Skin Frict.	Point Resist.	
From	To	Total	Subm.	Sep.	Accum.	Blows				$S=C+N\tan\phi$	$Pf = S \times H$	Sep.	Accum.
ft.	ft.	pcf	pcf	psi	psi	ft.	deg.		psi	psi	tsf	T/f*	T/f*
11(.072)12(2-1)													
0	8					27					.350	2.80	2.80
8	12					20		clay			.280	1.12	3.92
12	17					28					.363	1.82	5.74
17	20					21					.280	0.84	6.58
20	24					37					.489	1.96	8.54
24	28					28		clay			.373	1.49	10.03
28	30					** 40					.521	1.04	11.07
30	34					90					1.169	4.68	15.75
34	38					53					.695	2.78	18.53
38	42					11.75"					.758	3.03	21.56
42	46					3.0"					1.296	5.18	26.74
46	50					3.75"					1.296	5.18	31.92
50	54					5.25"					1.185	4.74	36.66
54	58					3.5"					1.296	5.18	41.84
58	59					7.25"					.869	0.87	42.71

*Tons per ft. of perimeter

Calculated by: H. F. Murray, Jr. Date: 6/15/71
Checked by: E. G. Doggett Date: 6/15/71

